NJC

ROYAL SOCIETY OF CHEMISTRY

PAPER

View Article Online
View Journal | View Issue

Cite this: *New J. Chem.*, 2021, 45, 13986

The antimicrobial potential and pharmacokinetic profiles of novel quinoline-based scaffolds: synthesis and *in silico* mechanistic studies as dual DNA gyrase and DHFR inhibitors†

Mohamed H. El-Shershaby,[a] Kamal M. El-Gamal,[a] Ashraf H. Bayoumi,[a] Khaled El-Adl,[bc] Mohamed Alswah,[a] Hany E. A. Ahmed,[ad] Ahmed A. Al-Karmalamy[e] and Hamada S. Abulkhair[*ae]

The resistance of pathogenic microbes to currently available antimicrobial agents has been considered a global alarming concern. Hence, close attention should be paid to the development of novel potent antimicrobials. Herein, we report the synthesis, *in vitro* antimicrobial evaluation, of two novel sets of quinoline derivatives as potential DNA gyrase and DHFR inhibitors. The design of new compounds depended on modifying the structural aspects of previously reported fluoroquinolones. In both sets, the methyl group replaced the fluorine atom at C-6. In the first set, the diverse heterocyclic fragments of reported antimicrobial potentials, including pyrazole, isoxazole, and pyrimidine, were attached to C-3 of the quinoline scaffold. In the second set, the quinolone ring was replaced with the pyrazolo [3,4-*b*]quinoline scaffold to examine the effect of this action on the antimicrobial activity and the *in silico* virtual binding with DNA gyrase and DHFR. The preliminary antimicrobial activity of new compounds was assessed against a panel of pathogenic microbes including Gram-positive bacteria (*Streptococcus pneumonia* and *Bacillus subtilis*), Gram-negative bacteria (*Pseudomonas aeruginosa* and *Escherichia coli*), and fungal strains (*Aspergillus fumigatus*, *Syncephalastrum racemosum*, and *Geotriucum candidum*). Six derivatives displayed relatively potent antimicrobial activity with a percent activity range of 80–113% relative to ampicillin, gentamicin, and amphotericin B as reference antimicrobial agents. Molecular docking studies were conducted to predict the binding affinities of new compounds toward the active sites of DNA gyrase and DHFR as proposed therapeutic targets.

Received 9th June 2021,
Accepted 5th July 2021

DOI: 10.1039/d1nj02838c

rsc.li/njc

1. Introduction

A wide-ranging panel of bacterial and fungal infections is becoming resistant to the effect of most frequently prescribed antibiotics and antifungal medications.[1,2] This resistance is the main obstacle to the management of infectious diseases. The World Health Organization has recognized this resistance and the dwindling number of present effective antimicrobial drugs as one of the alarming threats to human health.[3] Also, problems of vancomycin-resistant and methicillin-resistant *Staphylococcus aureus* (VRSA & MRSA), and fluconazole-resistant *Candida albicans* have reached a disturbing level worldwide.[4] Consequently, the battle is still on, and it is essential to develop new medications with improved antimicrobial potentials.

DNA gyrase enzyme (EC number: 5.6.2.2) is a topoisomerase II, that is crucial to DNA transcription and replication processes in eukaryotes.[5] Consequently, inhibition of DNA gyrase has long been considered as a striking goal for the development of antimicrobial agents against bacterial pathogens.[6,7] Quinolone antibiotics are the firstborn, and still the only, existing class of agents that have been clinically used to inhibit bacterial DNA synthesis.[8,9] Nalidixic acid, (**1**) is a quinolone that formed the basis for the development of improved analogues fluoroquinolone antibiotics. Fluoroquinolones and their analogous naphthyridines (Fig. 1) work as DNA gyrase poisons as they could inhibit bacterial

[a] *Pharmaceutical Organic Chemistry Department, Faculty of Pharmacy, Al-Azhar University, Nasr City 11884, Cairo, Egypt. E-mail: hamadaorganic@azhar.edu.eg*
[b] *Department of Medicinal Chemistry & Drug Design, Faculty of Pharmacy, Al-Azhar University, Cairo, Egypt*
[c] *Department of Pharmaceutical Chemistry, Faculty of Pharmacy, Heliopolis University for Sustainable Development, Cairo, Egypt*
[d] *Pharmacognosy and Pharmaceutical Chemistry Department, Pharmacy College, Taibah University, Al-Madinah Al-Munawarah 41477, Saudi Arabia*
[e] *Pharmaceutical Chemistry Department, Faculty of Pharmacy, Horus University - Egypt, International Coastal Road, 34518, New Damietta, Egypt*

† Electronic supplementary information (ESI) available. See DOI: 10.1039/d1nj02838c

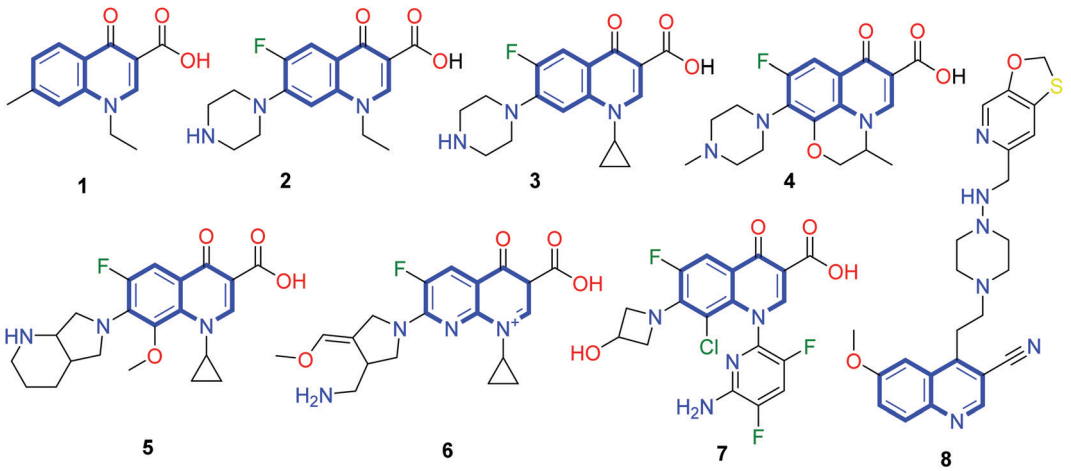

Fig. 1 Fluoroquinolones, analogous naphthyridine antibiotics and DNA gyrase/DHFR inhibitors.

nucleic acid synthesis,[8] thereby leading to cell death. Nowadays, the use of fluoroquinolones has a place in the management of serious microbial infections such as bacterial pneumonia[10] and urinary tract infections triggered by susceptible pathogens, including *E. Coli*, *Enterobacter*, and *Klebsiella* species.[11] Over time, the subsequent generations of novel fluoroquinolones with improved efficacy were developed namely: norfloxacin (**2**), ciprofloxacin (**3**), levofloxacin (**4**), moxifloxacin (**5**), gemifloxacin (**6**), and delafloxacin (**7**). In addition, GS-K299423 (**8**) is mechanistically distinct from fluoroquinolones, which has recently been reported as a bacterial topoisomerase type II inhibitor and showed a potent inhibitory effect on DNA gyrase supercoiling in *Streptococcus aureus*.[12] Furthermore, the design of quinolines over the last few years as antimicrobial and anticancer agents is continuing and provides new derivatives with interesting activities.[13,14]

On the other hand, pathogenic fungi are one of the most harmful parasitic organisms that can cause serious health problems. Fungal infections also produce various toxins that cause critical health problems, including disability and death.[15] Like bacteria, fungi can develop resistance when fungi are able to defeat drugs designed to exterminate them. Over the last few decades, the misuse of antifungal medications has triggered a resistance to eradicate fungi, creating the efficacy of current traditional fungicides decline. Consequently, it is also essential to develop novel effective fungicides to control those fungal diseases.

The dihydrofolate reductase (DHFR; EC number: 1.5.1.3) is an essential enzyme for the conversion of folic acid to its reduced form, tetrahydro-folic acid (THF). The inhibition of DHFR interrupts the biosynthesis of THF, which is crucial for the growth of both bacteria and fungi. Therefore, DHFR inhibition has long been a remarkable goal for the development of antimicrobial agents against both pathogen types.[16] Over the last decade, there were several reports on novel quinoline derivatives as potential antimicrobial agents that target DNA gyrase and DHFR.[7,13,17,18] However, continuing bacterial and fungal resistance to present antimicrobials with no novel medications in the antimicrobial pipeline has driven intensive research in this area.

Quinoline is a vital pharmacophore ring system, presented in a number of antifungal agents.[17,19] Additionally, quinoline derivatives possess a diverse pharmacological activity, particularly as antimalarial,[20,21] anticancer,[22,23] antibacterial,[6,7,17] and antifungal.[17,18,24]

Other pharmacophoric heterocyclic ring systems are embedded in the core structures of reported antimicrobials with DNA gyrase and/or DHFR degrading effect *viz.* pyrazole,[25–27] isoxazole,[28–30] and pyrimidine.[31,32] All the latter heterocyclic moieties were reported to have the optimum spatial configurations that enable them to interact with the DNA gyrase binding site.[33–35] Moreover, the α, the β-unsaturated ketonic fragment is also presented in a number of synthetic derivatives with potent antimicrobial and DNA gyrase inhibitory activity.[27,36,37] Hybrid molecules constructed by joining more than one pharmacophore may exert better activity than the individual activity of each isolated one.[38,39]

1.1. Rationale and aim of the work

Based on the aforementioned facts, inspired by the versatility of the quinoline moiety as an essential fragment in many FDA-approved antimicrobial agents, and in continuation of our recent studies[30,40,41] of identifying new antimicrobial agents, syntheses of novel sets of 2-chloro-6-methylquinolin and 6-methyl-1*H*-pyrazolo[3,4-*b*]quinoline derivatives were carried out (Fig. 2) to get new molecules with good antimicrobial potency. The design of new compounds depended on modifying structural aspects of the previously reported fluoroquinolones to evaluate their activities against pathogenic bacterial and fungal strains. In the first set of compounds, methyl group replaced the fluorine atom, and diverse heterocyclic fragments of reported antimicrobial potentials, including pyrazole,[17,25] isoxazole,[28,42] and pyrimidine,[31,32,43] were attached to C-3 of the quinoline scaffold to investigate the effect of such substitution pattern on the antimicrobial activity of the designed compounds. In the second set, the quinolone ring was replaced with a pyrazolo[3,4-*b*] quinoline scaffold to which a number of other pharmacophoric tails were linked to C-3. All the synthesized compounds were

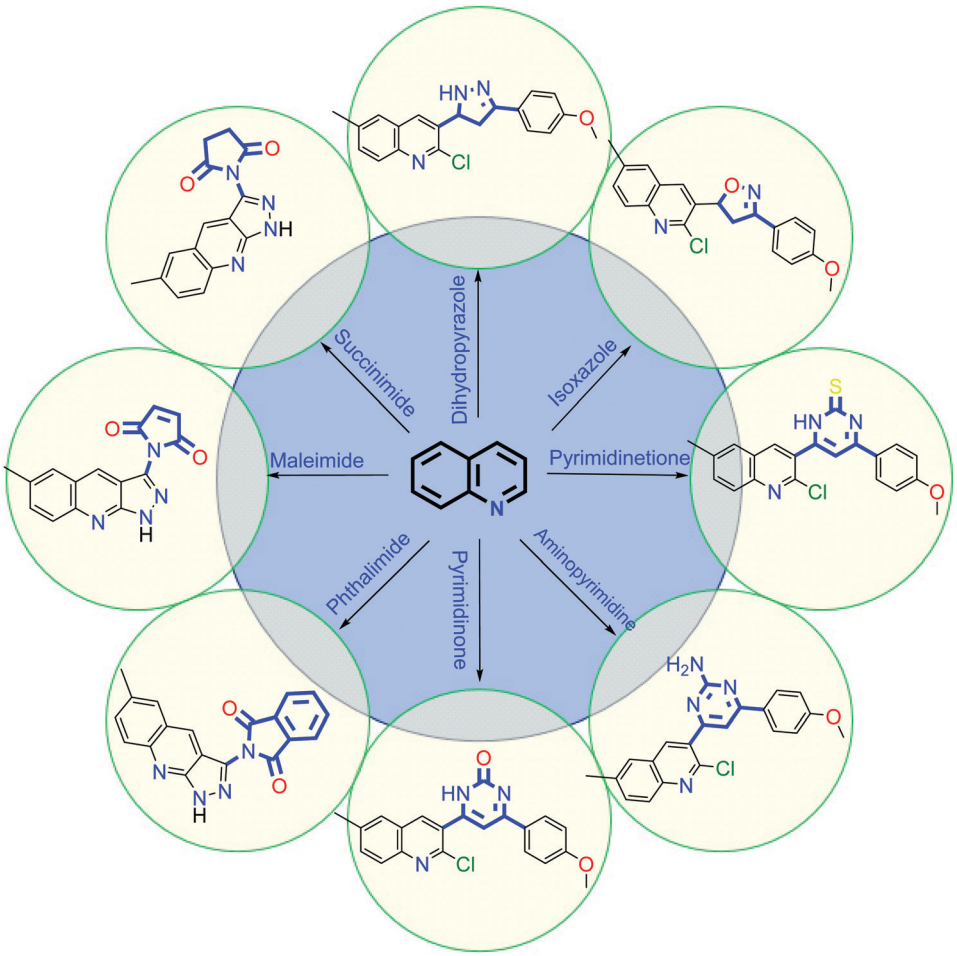

Fig. 2 Rational design of the new pharmacophore-linked quinolines.

evaluated for their *in vitro* antimicrobial activity against a panel of pathogenic microbes including Gram-positive bacteria (*Streptococcus pneumonia* and *Bacillus subtilis*), Gram-negative bacteria (*Pseudomonas aeruginosa* and *Escherichia coli*), and fungal strains (*Aspergillus fumigatus*, *Syncephalastrum racemosum*, and *Geotriucum candidum*). In addition, the structure–activity relationship of the new compounds is discussed. As well, a subsequent molecular docking study of the most active compounds was carried out to predict the binding affinity toward the active site of DNA gyrase/DHFR enzymes as proposed therapeutic targets of their antimicrobial activity. Furthermore, ADMET profiles of the highest effective derivatives were examined to evaluate the potential of new compounds to build up as good drug candidates.

2. Results and discussion

2.1. Chemistry

Synthetic approaches adopted for the synthesis of the starting 2-chloro-6-methylquinoline-3-carbaldehyde (**9**) and 6-methyl-1*H*-pyrazolo[3,4-*b*]quinolin-3-amine (**11**) are presented in Scheme 1. In the present work, Vilsmeier-Haack method[44] was selected to prepare the first intermediate **9**. Quinolin-3-

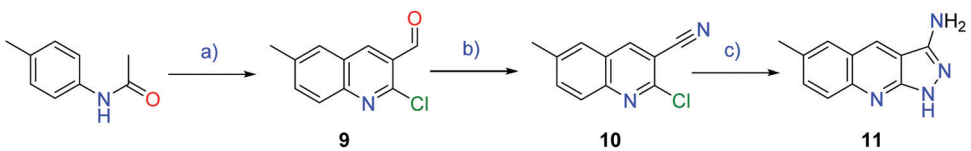

Reagents and Conditions

a) $POCl_3$/DMF, 0 °C, 8 h, 72%; b) $NH_2OH.HCl$, 120 °C, 8 h, 80%; c) $NH_2NH_2.H_2O$, 120 °C, 12 h, 65%

Scheme 1 Synthetic protocol of starting quinoline and pyrazoloquinoline derivatives.

carbaldehyde derivative **9** was employed as a starting material for the synthesis of the chalcone **12** and subsequent binucleophilic addition reaction products **13–17**. Compound **10** was obtained in good yield (80%), adopting Bell and Ackerman-modified protocol,[45] where compound **9** was treated with hydroxylamine hydrochloride at 70 °C for 2 h. Then, the *in situ* formed oxime was directly heated up to 110 °C to lose a water molecule and give the desired quinoline-3-carbonitrile product. Treating the carbonitrile derivative **10** with hydrazine hydrate[23,46,47] gave 6-methyl-1*H*-pyrazolo[3,4-*b*]quinolin-3-amine (**11**), which was used as a starting material in the synthesis of final pyrazoloquinoline derivatives (**18–22**).

As depicted in Scheme 2, our convergent synthesis approach of final compounds **12–17** started with the preparation of 3-(2-chloro-6-methylquinolin-3-yl)-1-(4-methoxyphenyl)prop-2-en-1-one by means of Claisen condensation of the aldehyde derivative **9** with *p*-methoxyacetophenone in the presence of sodium hydroxide.[48–50] The produced chalcone was treated with a set of five different binucleophiles in a series of binucleophilic addition reactions to obtain the final new compounds **13–17**.

The structure of chalcone **12** was established based on its elemental and spectral data. The IR spectrum is characterized by the presence of a strong absorption band at 1655 cm^{-1} due to carbonyl ketone stretching, which appeared at a low absorption value because of extended alkene conjugation with the carbonyl double bond. The absolute geometry of the α,β-unsaturated carbonyl linker was assigned to be in the *trans* form based on the coupling constant of alkene protons (*J* value = 15.0 Hz). In the present work, five different binucleophilic addition reactions have been achieved. Namely, chalcone **12** was allowed to react with hydrazine hydrate, hydroxylamine hydrochloride, thiourea, guanidine hydrochloride and urea. In general, all reactions proceeded smoothly, and final products were obtained in relatively good yields as detailed in the experimental part. First, to build a dihydropyrazole ring system, a mixture of chalcone **12** was heated up with hydrazine hydrate at reflux temperature to give the desired dihydropyrazole **13**. The structure of **13** was established on the basis of its elemental and spectral data. The important band in the IR spectrum of compound **13** was revealed at 3290 cm^{-1} due to NH stretching of the newly formed dihydropyrazole ring. The later NH also appeared on the ^1H NMR spectrum as a broad D_2O-exchangeable singlet within the aromatic region at 7.6 ppm. As well, the disappearance of the conjugated α, β-unsaturated carbonyl characteristic absorption band at 1655 cm^{-1} confirmed the proposed structure of **13**. Furthermore, the appearance of three new signals in the ^1H NMR spectrum at δ 15.3, 3.6, and 2.9 corresponding to pyrazole-H5, pyrazole-H4

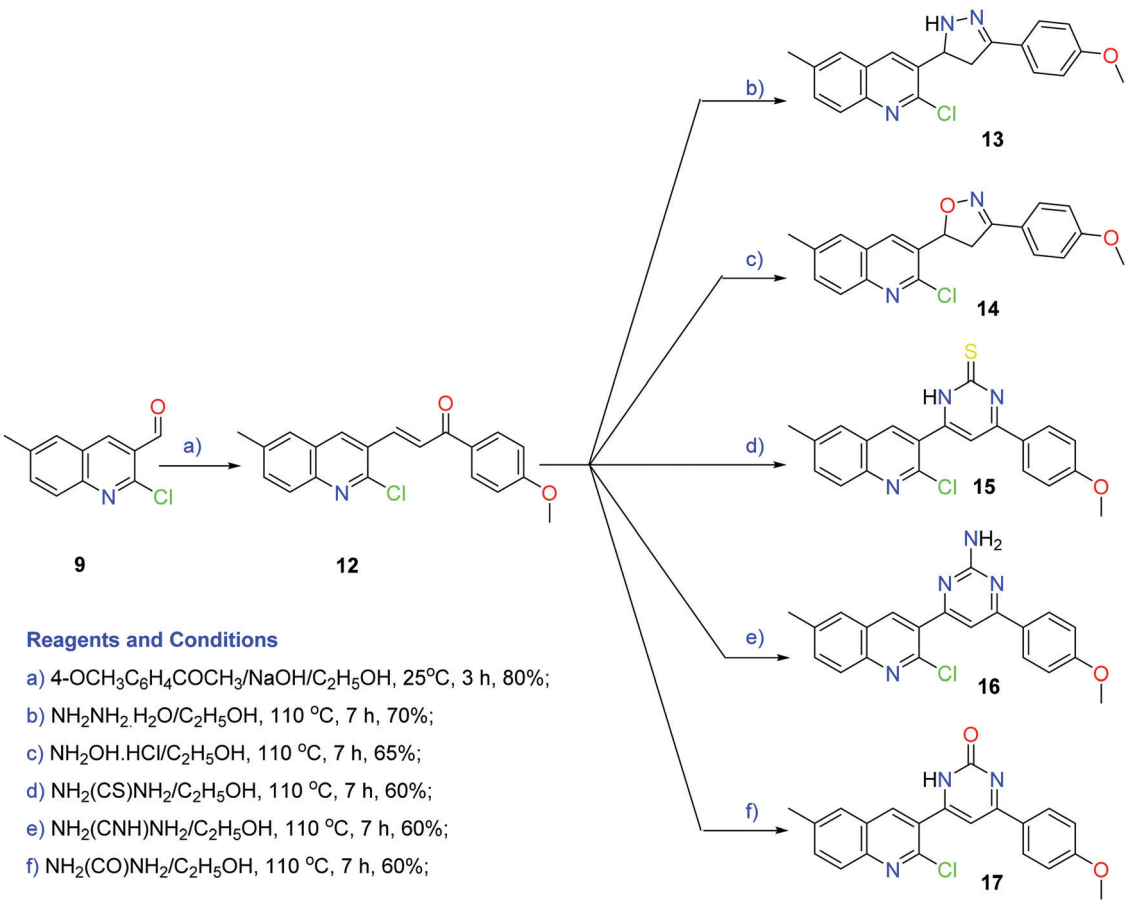

Scheme 2 Synthetic route of new quinoline derivatives **12–17**.

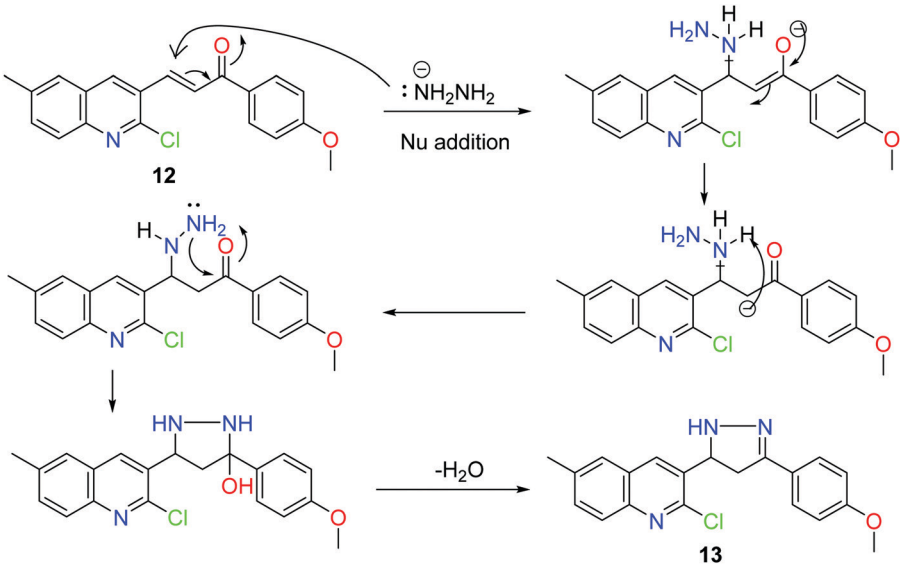

Chart 1 The proposed mechanism for construction of compound **13**.

axial and equatorial protons, respectively, further confirmed the structure. Collectively, the formation of the binucleophilic addition reaction products **13–17** was postulated to pass through two steps. The formation of **13**, as a representative example, includes in the first step a Michael-type addition on the carbonyl β-carbon, followed by protonation to afford β-hydrazinylpropanone intermediate. In this cyclization reaction, the hydrazine nucleophile is firstly attacking the carbonyl β-carbon of chalcone **12**. A subsequent protonation of the anionic α-carbon takes place to restore the trivalent state of nitrogen of the formed hydrazinium transition state. The terminal amino group is then attacking the carbonyl carbon of the chalcone while carbonyl oxygen gets hydroxylated. The unsaturation is finally located between the carbonyl carbon and the adjacent α carbon *via* the elimination of a water molecule, as revealed in Chart 1.[51–53]

Next, to synthesize 2-chloro-3-[3-(4-methoxy-phenyl)-4,5-dihydro-isoxazol-5-yl]-6-methyl-quinoline (**14**), a mixture of chalcone **12**, hydroxylamine hydrochloride and NaOH in ethanol was heated to reflux to give the desired compound according to the reported procedure [17]. The spectral data of the isolated product confirmed structure **14**, the ^{1}H NMR spectrum showed a triplet of one proton at 5.7 ppm due to isoxazole-H5, which appeared downfield as expected because C-5 of isoxazole is attached to the oxygen atom, two doublets of the doublet, each equivalent for one proton at 4.0 ppm and 3.6 ppm, which are attributed to isoxazole-H4 axial and equatorial protons, respectively. The most characteristic observation in the ^{1}H NMR spectrum of compound **14** is the disappearance of the olefinic protons of chalcone **12**.

Afterward, to prepare pyrimidine-2-thione derivative **15**, a mixture of chalcone **12**, thiourea and NaOH in ethanol was heated to reflux. The IR spectrum is characterized by an absorption band at 3290 cm^{-1} assignable to one NH stretching; the ^{1}H NMR spectrum showed a singlet of one proton at 11.98 ppm due to NH, which is D_2O exchangeable, a singlet of three protons at 3.8 ppm due to OCH_3 of phenyl and a singlet of three protons at 2.36 ppm due to CH_3 of quinoline. Similarly, chalcones were reported to react with guanidine hydrochloride, giving the corresponding 2-aminopyrimidines.[30] According to this procedure, 4-(2-chloro-6-methylquinolin-3-yl)-6-(4-methoxyphenyl) pyrimidin-2-amine (**16**) was synthesized. The structure of the isolated product was confirmed by spectral data, the IR spectrum characterized by a band at 3300 cm^{-1} due to NH_2 stretching. The latter amino group at C-2 of the pyrimidine ring presented a D_2O-exchangeable singlet signal at δ 6.6 in the ^{1}H NMR spectrum.

Unlike the previous four reactions in this series, a reaction with urea preceded first under basic conditions, but the yield was poor, therefore we shifted towards the acidic medium. In brief, 6-(2-chloro-6-methylquinolin-3-yl)-4-(4-methoxyphenyl)pyrimidin-2(1*H*)-one (**17**) was prepared, in a good yield, by allowing chalcone **12** to react with urea in the presence of conc. hydrochloric acid at a reflux temperature. Under strong acidic media, an alternative product was also anticipated, where the 2-chloroquinoline was expected to be alternatively hydrolyzed to afford the amide-containing structure (Chart 2)).[54,55] The later structure was excluded based on the absence of its molecular ion peak from the MS and the absence of a characteristic isotopic pattern of chlorine-containing compounds. Other spectral and elemental data confirmed this assumption and confirmed the structure of compound **17**.

Scheme 3 shows the adopted synthetic routes for the preparation of new pyrazoloquinoline derivatives. The approaches depended on the nucleophilic condensation reaction of 6-methyl-1*H*-pyrazolo[3,4-*b*]quinolin-3-amine with different acid anhydrides and acid halides.[77] Chemical structures of isolated compounds **18–22** were assigned based on their spectral and elemental analyses. For instance, the lack of the biforked band characteristic to the primary amine of the starting material, compound **11**, from all IR spectra, confirms the consumption of the aminopyrazoloquinoline and the reaction preceded to the completion. In addition, the appearance of a band corresponding to an

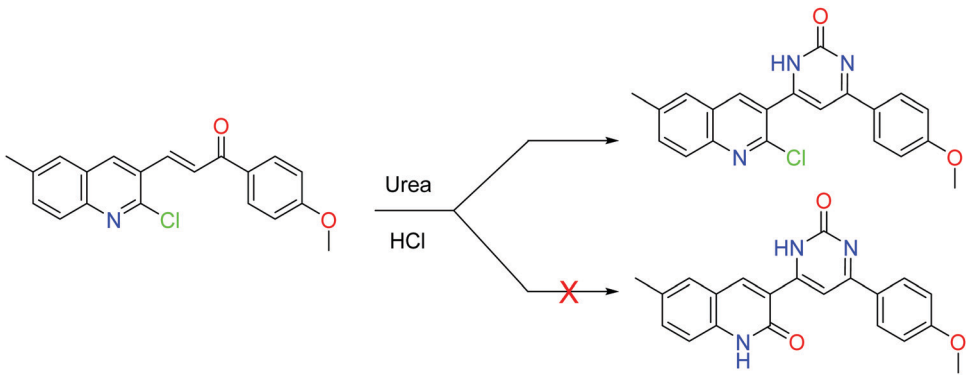

Chart 2 Anticipated products upon the reaction of chalcone **12** with urea under acidic conditions.

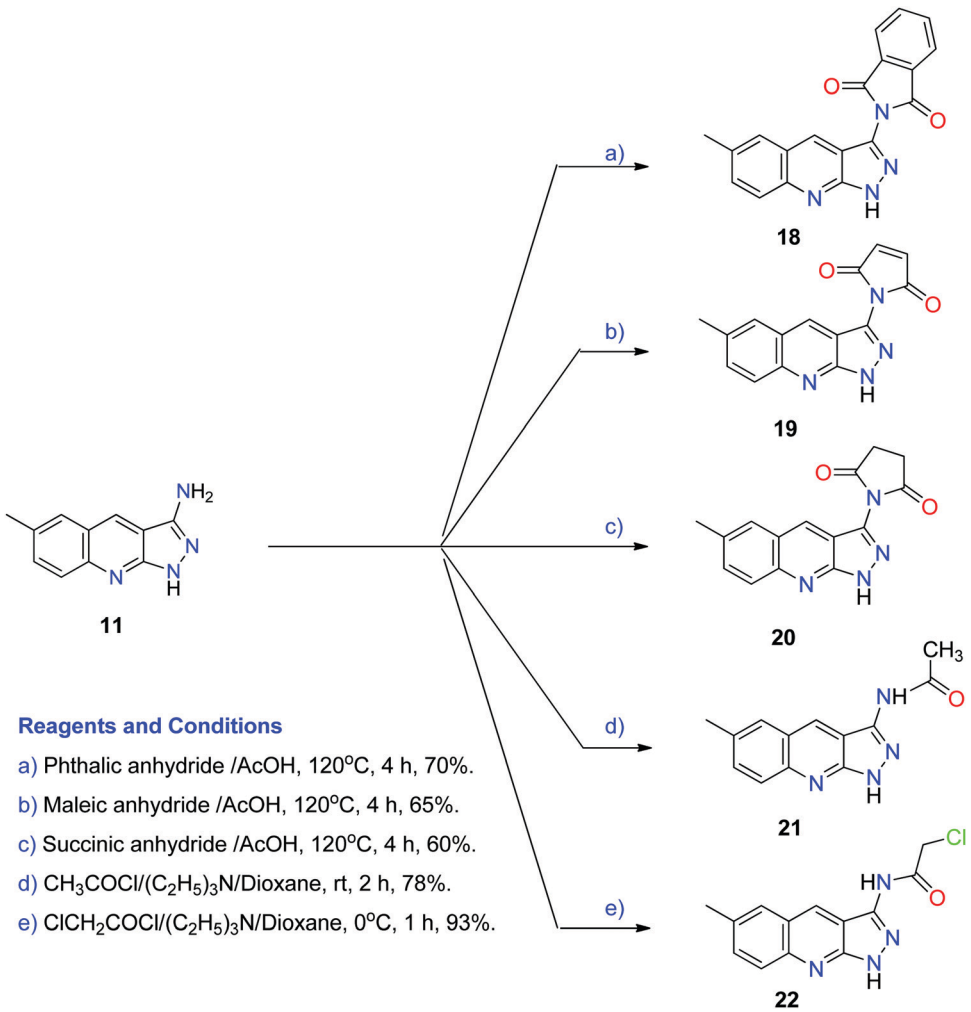

Scheme 3 Synthetic route of new pyrazoloquinoline derivatives **18–22**.

amide carbonyl group between 1664 and 1683 cm^{-1} also verifies tethering the new entity with the aminopyrazole ring of the starting compound.

The progress of all chemical reactions was validated by TLC methodology and final products were purified by column chromatography method. Structures and purity of new derivatives were confirmed based on their IR, LC-MS, ^1H NMR, and ^{13}C NMR spectral data.

2.2. Evaluation of biological activity

2.2.1. Antibacterial activity. All the newly synthesized compounds were evaluated for their *in vitro* antibacterial activity

against four bacterial pathogens: *Streptococcus pneumonia* and *Bacillus subtilis* as examples of Gram-positive bacteria; *Pseudomonas aeruginosa* and *Escherichia coli* as examples of Gram-negative bacteria. Results of the antibacterial activity of new compounds are presented in Table 1. Agar-diffusion method[56] was used for the preliminary evaluation of antibacterial activity following the directions of the Clinical and Laboratory Standards Institute and results were listed as the average diameter in mm of inhibition zones (IZs) of bacterial growth. Ampicillin and gentamycin were used as standard references for Gram-positive and Gram-negative bacteria, respectively.

2.2.2. Antifungal activity. The synthesized compounds were tested *in vitro* for antifungal activity against three fungal pathogenic strains: *Aspergillus fumigatus*, *Syncephalastrum racemosum*, and *Geotriucum candidum.* The Agar-diffusion method[56] was also used for the evaluation of the tentative screening of antifungal activity. Amphotericin B and DMSO were used as positive and negative controls, respectively. Results for each test compound were recorded as the average of inhibition zone diameter in mm of fungal growth. Inhibition zone diameters of the test compounds and amphotericin B are shown in Table 2.

2.2.3. Structure–activity relationship study. From the above-tabulated data, it is clear that the inhibition zone diameters obtained for the new compounds revealed the significant antimicrobial activity of new compounds against tested microbial pathogens. Most of the studied derivatives presented a better activity toward the Gram-positive than that of Gram-negative strains. As expected, there were no significant variations between the antimicrobial activity of derivatives incorporating more than one pharmacophoric ring system (**13–17**). On the other hand, there is a noted variation in the potency between the pyrazoloquinolines derivatives. Inhibition zones in the antifungal activity evaluation revealed the same trend as that of the antibacterial activity.

Analyzing the antibacterial activity of derivatives with more than one pharmacophoric ring system **13–17** revealed that the best activity against *Streptococcus pneumonia* and *Bacillus subtilis* was observed in the case of the aminopyrimidine derivative **16** with activity percentages of 102% and 80%, respectively, compared with ampicillin. This finding could be supported by the documented potentials of analogous aminopyrimidines as modulators of bacterial biofilm formation[57] and as an antibacterial against *Staphylococcus aureus*, *Bacillus subtilis*, *Escherichia coli*, and *Pseudomonas aeruginosa*.[58] The highest potency against Gram-negative strain, *Escherichia coli*, was obtained by the action of the pyrimidin-2-thione **15**, which presented an equipotent activity with that of gentamicin. 2-Amino-4,6-disubstituted pyrimidines and pyrimidine-thiones were previously reported as effective antibacterials against Gram-negative strains, such as *Pseudomonas aeruginosa* and *Escherichia coli*.[59] Regarding the antibacterial activity of the pyrazoloquinoline derivatives **18–22**, the best activity against Gram-positive bacterial strains, *Streptococcus pneumoniae* and *Bacillus subtilis* were observed in the case of the ketonic derivatives **21** and **22** with activity percentages of 112% and 86% respectively (for compound **21**) and 95% and 83%, respectively, (for compound **22**) compared with that of the positive control. The highest potency against Gram-negative strain, *Escherichia coli*, was gained under the effect of the halogenated ketonic derivative **22**, which showed a much better activity than that of gentamicin (109%). Unfortunately, there was no detected activity against *Pseudomonas aeruginosa* with any of the tested compounds. The assessment of halogenated quinolines as antibacterial and biofilm-exterminating agents was reported in several studies. Halogenated quinolines demonstrated more potent antibacterial activity than nitroxoline against *Staphylococcus. aureus* and *Staphylococcus* epidermidis strains.[60]

Regarding the antifungal activity, the tabulated results revealed moderate to good activity for most of the new derivatives. Compounds **15**, **16**, **20**, **21**, and **22** were the most potent with either an equipotent or even higher potency than that of the standard drug. The highest potent compound against *Aspergillus fumigatus* was **20** followed by **16** with efficacy percentages of 102% and 97%, respectively, compared with amphotericin-B.

Table 1 Antibacterial activity of new compounds against Gram-positive and Gram-negative pathogens

Cpd no.	Inhibition zone[a] (mm)			
	Streptococcus pneumoniae	*Bacillus subtilis*	*Pseudomonas aeruginosa*	*Escherichia coli*
12	16.2 ± 0.15	19.8 ± 0.42	NA[b]	15.3 ± 0.53
13	16.3 ± 1.2	18.2 ± 2.1	NA	15.4 ± 0.72
14	**19.3 ± 0.58**	**21.2 ± 0.72**	NA	**NA**
15	**21.3 ± 0.44**	**22.1 ± 0.63**	NA	**21.2 ± 0.58**
16	**24.3 ± 2.1**	**26.2 ± 0.58**	NA	**18.6 ± 0.72**
17	**19.3 ± 0.58**	**21.2 ± 0.72**	NA	NA
18	16.8 ± 0.58	19.1 ± 0.63	NA	15.6 ± 0.63
19	17.1 ± 1.5	19.6 ± 0.63	NA	16.3 ± 0.72
20	16.3 ± 1.5	18.1 ± 0.58	NA	14.8 ± 2.1
21	**26.8 ± 1.63**	**28.1 ± 0.58**	NA	**22.3 ± 1.5**
22	**22.8 ± 2.1**	**26.8 ± 0.58**	NA	**23.4 ± 0.63**
Ampicillin	23.8 ± 0.2	32.4 ± 0.58	NT[c]	NT
Gentamicin	NT	NT	17.3 ± 0.63	21.3 ± 0.58

[a] Mean zone of inhibition in mm ± standard deviation for three experiments. [b] NA = no activity. [c] NT = not tested.

Table 2 Antifungal activity of new compounds

Cpd no.	Inhibition zone[a] (mm)		
	Aspergillus fumigatus	*Syncephalastrum racemosum*	*Geotriucum candidum*
12	**20.1 ± 1.2**	**18.3 ± 0.58**	**20.1 ± 2.1**
13	15.7 ± 0.33	15.9 ± 0.25	16.8 ± 0.34
14	**18.3 ± 1.2**	**19.3 ± 0.58**	**20.4 ± 2.1**
15	**19.8 ± 1.2**	**20.5 ± 0.25**	**21.4 ± 0.58**
16	**23.2 ± 0.58**	**21.4 ± 1.5**	**24.6 ± 0.44**
17	16.3 ± 1.2	14.2 ± 0.58	15.9 ± 2.1
18	16.9 ± 0.63	15.2 ± 1.2	16.3 ± 0.42
19	14.6 ± 1.5	13.4 ± 0.44	15.4 ± 1.2
20	**24.2 ± 0.58**	**22.3 ± 1.2**	**27.3 ± 0.58**
21	**22.3 ± 1.2**	**20.7 ± 0.58**	**25.2 ± 0.63**
22	17.3 ± 2.1	16.4 ± 0.58	19.1 ± 1.5
Amphotricin B	23.7 ± 0.63	19.7 ± 0.72	28.7 ± 0.58

[a] Mean zone of inhibition in mm ± standard deviation for three experiments.

Pyrrolidinedione incorporating derivatives were previously recognized as potent antifungal strains such as *Aspergillus fumigatus*.[61] The same activity pattern was observed against *Syncephalastrum racemosum*, where compounds **20** and **16** showed a more potent antifungal activity than the standard drug with efficacy percentages of 113% and 108%, respectively. Also, the succinimide derivative **20** revealed the best activity against the last tested fungal species, *Geotriucum candidum* with an equipotent activity with that of the standard antifungal agent. A graphical summary of the structure–activity relationship of the most active derivatives compared with standard antimicrobial agents is presented in the ESI.† A graphical summary of the structure–activity relationship of the most active derivatives compared with standard antimicrobial agents is presented in Charts 3 and 4.

2.2.4. Molecular docking study. DNA gyrase and DHFR have been defined as molecular targets for the antibacterial[6,7,62] and antifungal activity[16,63,64] of quinoline derivatives, respectively. Accordingly, they were selected for computational studies to rationalize the mechanism of action of the five most active compounds. Based on PDB search for *E coli* DNA gyrase and *Aspergillus flavus* DHFR, fifteen protein codes were obtained for the former and two codes for the latter. Based on the obtained docking score values, 4DUH and 6DTC complexes were selected for molecular docking studies to understand the proposed binding interactions of the highest active compounds inside the pockets of *Escherichia coli* DNA gyrase (EC number: 5.6.2.2) as a target for antibacterial activity[65] and *Aspergillus flavus* dihydrofolate reductase (EC number: 1.5.1.3) as a target for antifungal activity.[66] The *in silico* docking studies were performed using the MOE software, employing the flexible docking protocol implemented in the MOE software. Docking studies were validated in terms of the root mean square deviation (RMSD). Poses possessing RMSD values within 0–1.20 Å were only considered.[67]

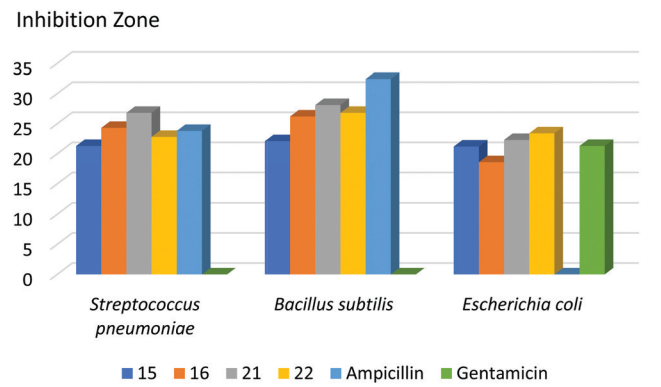

Chart 3 A graphical comparison between the inhibition zones of compounds **15**, **16**, **21**, and **22** and standard drugs against three of tested bacterial strains.

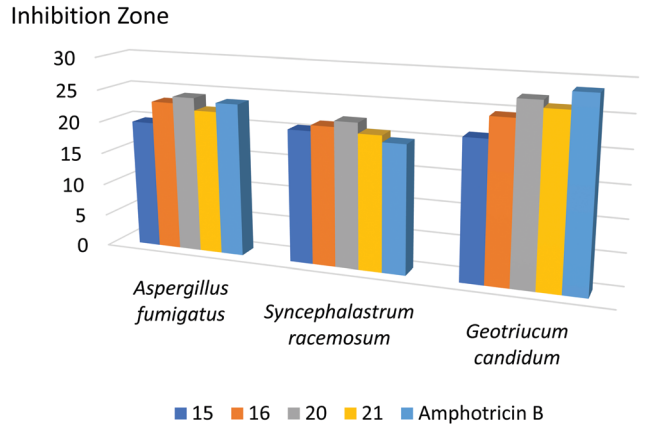

Chart 4 A graphical comparison between the inhibition zones of compounds **15**, **16**, **20**, and **21** and the standard drug against tested fungal strains.

2.2.4.1. Docking against Escherichia coli DNA gyrase. With two main interactions, the binding mode of the initial ligand, RLI[65] with the active pocket of DNA gyrase, exhibited binding energy of −13.85 kcal mol^{-1} (Fig. 3). These interactions include (**a**) two hydrogen-bonding interactions between the carboxylate group of RLI and both Arg76 and Arg136 residues; (**b**) another two hydrogen bonds between NH and the S atom of the thiazole ring of RLI and GLY101 residue. Free energy of binding, hydrophobic interactions, and H-bonding interactions of the highest potent derivatives (**15**, **16**, **20**, **21**, and **22**) and that of RLI are presented in Table 3.

The behavior of new quinoline derivatives in the DNA gyrase binding pocket is summarized in Fig. 4 and 5 and is almost like that of RLI. The binding mode of compound **15** exhibited an affinity value of −10.98 kcal mol^{-1} and almost obeyed the same interaction pattern of RLI with the binding site of DNA gyrase. The chlorine atom of **15** formed a hydrogen bond with ILE94 residue within 3.51 Å. Three additional hydrophobic interactions are formed between the quinoline ring scaffold and the PRO79, LYS103, and ASN46 residues (Fig. 4 and 5). These four desirable noncovalent interactions of compound **15** might explain the superior activity of such a derivative as an antimicrobial agent. The aminopyrimidine derivative **16** revealed an affinity value of −10.96 kcal mol^{-1} and exhibited a different virtual binding mode with the DNA gyrase enzyme. The quinoline ring of compound **16** played as a backbone HB acceptor to form two hydrogen bonds with GLY101 and GLU50 residues. Also, the latter derivative exerted two hydrophobic interactions with the amino acid residues PRO79 and LYS103. The pyrrolidine-dione

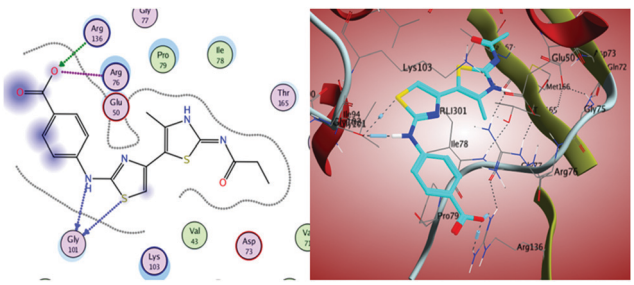

Fig. 3 2D and 3D interactions of the internal ligand, with the active site of DNA gyrase.

Table 3 Results of *in silico* docking for the most active compounds

Comp.	ΔG (kcal mol^{-1})	RMSD (Å)	H-Bonding interactions: Residue	H-Bonding interactions: Distance (Å)	Hydrophobic interactions: Residue	Hydrophobic interactions: Distance (Å)
			ARG76	3.06		
RLI	−12.23	0.91	ARG136	3.15	—	
			GLY101	3.63		
			GLY101	2.81		
15	−10.98		ILE94	3.51	PRO79	3.97
		1.00			LYS103	3.98
					ASN46	3.71
16	−10.96	1.01	GLY101	3.27	PRO79	3.83
			GLU50	3.56	LYS103	3.97
20	−11.21		THR165	3.10	LYS103	3.88
		0.52	LYS103	2.84		
			VAL120	3.40		
21	−10.33		ASP73	2.94	ILE78	4.53
		1.17			ILE78	3.99
					PRO79	3.61
					LYS103	4.04
22	−10.71	1.07	ASP73	2.90	LYS103	3.93

derivative **20** revealed a much better affinity value, (−11.21 kcal mol^{-1}), and showed four different interaction patterns with the binding site of the DNA gyrase receptor. These interactions involve three hydrogen bonds between both oxygens of the pyrrolidine-dione moiety and the quinoline ring of the target compounds with THR165, LYS103, and VAL120 residues, respectively. The fourth interaction is in the form of arene-H hydrophobic interaction between the benzene ring of the quinoline scaffold and the LYS103 residue. With −10.33 and −10.71 kcal mol^{-1} free energies of binding, the obtained docking results for the carbonyl-containing derivatives **21** and **22** involve one hydrogen bonding between the secondary amide functionality in the target compounds and the amino acid residue ASP73. Quinoline rings of both the latter compounds presented a hydrophobic interaction with LYS103 residue. Distinguishably, compound **21** showed three additional arene-H hydrophobic interactions with amino acid residues ILE78, ILE78, and PRO 79.

2.2.4.2. Docking against Aspergillus flavus dihydrofolate reductase. The molecular docking study of the five most active synthesized quinolines was performed against the three-dimensional structure of Dihydrofolate Reductase (DHFR) of *Aspergillus flavus* to realize their binding affinity and interactions with the potential enzyme target of their antifungal activity. New ligands and the internal co-crystallized one (H9G) were docked in the active site of modeled DHFR. The binding mode of the redocked ligand, H9G with the pocket of *Aspergillus flavus* DHFR enzyme, demonstrated binding energy of −11.16 kcal mol^{-1}. There are two main interactions between H9G and the receptor-binding site (Fig. 6): (**a**) two hydrogen-bonding interactions between the amino group at position 9 of the 2,3-dihydrofuro[2,3-*f*]quinazoline ring and N-3 of tetrazole ring in H9G and ILE10 and ARG80 residues, respectively; (**b**) an arene-H interaction between the tetrazole ring of H9G and the amino acid residue LEU77. An outline of free energy of binding, H-bonding interactions, and hydrophobic interactions of selected compounds and that of the internal co-crystallized ligand is shown in Table 4.

The behavior of new quinoline derivatives in the *Aspergillus flavus* DHFR binding pocket is summarized in Fig. 7 and 8 and is almost similar to that of H9G. The binding mode of compound **15** exhibited an affinity value of −10.29 kcal mol^{-1}. The methoxyphenyl moiety of **15** presented a desirable π–π stacking with PHE44 residue and occupied the hydrophobic pocket formed by ILE10, ILE156, ALA12, VAL11, ASP40, MET41, and THR66. The NH of the pyrimidine ring played as a hydrogen bond donor with the amino acid residue SER69. In addition, an arene-H interaction within 4.15 Å is formed between the quinoline ring and the amino acid residue VAL70. Similarly, obeying the same interaction pattern and occupying

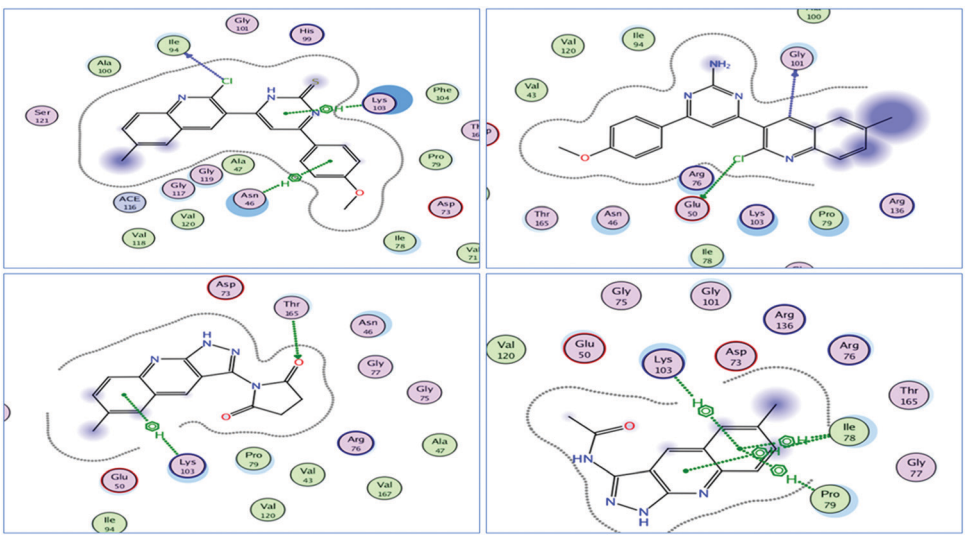

Fig. 4 2D interactions of compounds **15** (upper left panel), **16** (upper right panel), **20** (lower left panel), and **21** (lower right panel) with the active site of DNA gyrase enzyme.

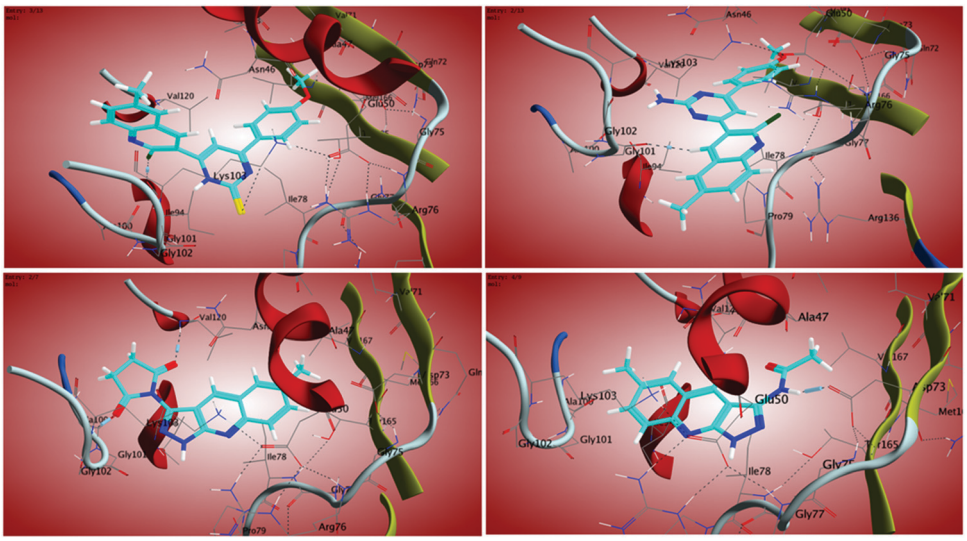

Fig. 5 3D interactions of compounds **15** (upper left panel), **16** (upper right panel), **20** (lower left panel), and **21** (lower right panel) with the active site of DNA gyrase enzyme.

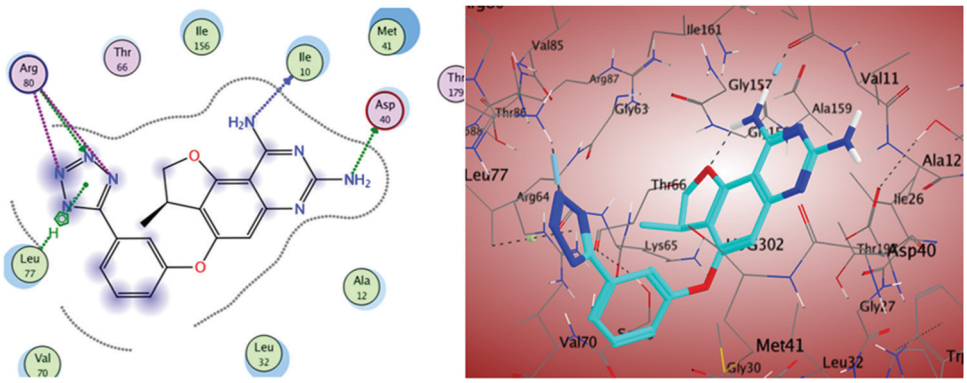

Fig. 6 2D and 3D interactions of H9G with the active site of Aspergillus flavus DHFR.

the same pocket, the binding mode of compound **16** exhibited an affinity value of −11.11 kcal mol^{-1}. The primary NH_2 group played as a hydrogen bond donor with SER69 residue. Additional two arene–H interactions within distances of 4.02 and 4.57 Å are formed between the pyrimidine and quinoline rings of **16** and the amino acid residues LEU32 and VAL70, respectively. With no hydrogen bonding interaction, the pyrrolidine-dione derivative **20** revealed an affinity value of −8.83 kcal mol^{-1} and exhibited a different virtual binding mode with the DHFR active site. The quinoline and pyrazole rings of compound **20** displayed two arene–H interactions within distances of 4.43 and 3.90 Å between the quinoline and pyrazole rings and the amino acid residues LEU32 and VAL70, respectively. With −8.75 and −8.45 kcal mol^{-1} free energies of binding, respectively, the obtained docking results for the ketonic derivatives **21** and **22** involved one hydrogen bonding between the NH of pyrazole ring in the target compounds and the amino acid residue TYR162. An additional arene-H interaction formed between the pyrazole ring of each compound and the GLY157 residue.

Table 4 Results of docking for the most active compounds with the binding site of DHFR

			H-Bonding interactions		Hydrophobic interactions	
Comp.	ΔG (kcal mol^{-1})	RMSD (Å)	Residue	Distance (Å)	Residue	Distance (Å)
H9G	−11.16	1.03	SER69	2.99	VAL70	4.15
15	−10.29	1.18	SER69	2.99	VAL70	4.15
16	−11.11	1.09	SER69	2.80	LEU32	4.02
					VAL70	4.57
20	−8.83	0.52	—	—	LEU32	4.43
					VAL70	3.90
21	−8.75	0.94	TYR162	3.08	GLY157	4.45
22	−8.45	1.02	TYR162	2.98	GLY157	3.16

2.2.5. Pharmacokinetic study. In the present work, a computational study was conducted on compounds showing the best antimicrobial activity to determine their main physico-chemical properties according to the directions of Lipinski's

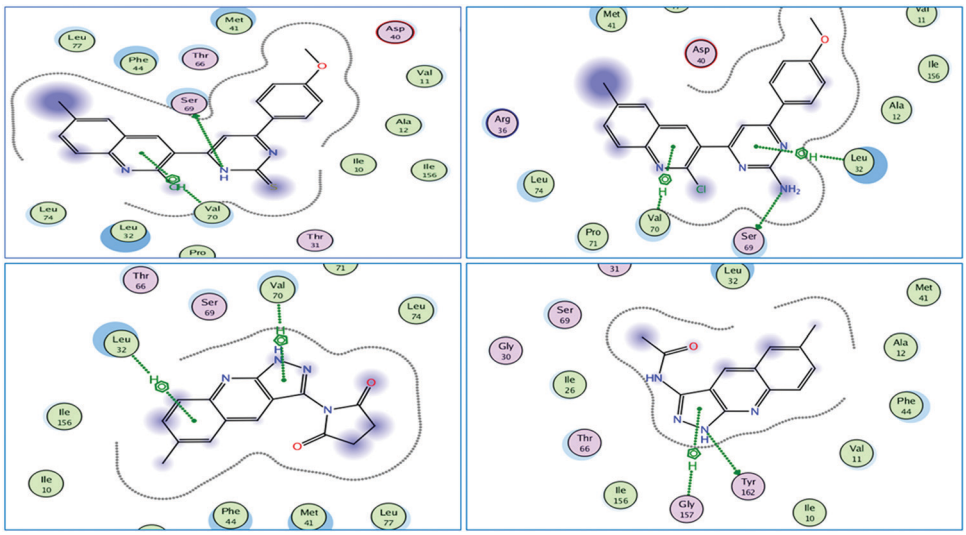

Fig. 7 2D interactions of compounds **15** (upper left panel), **16** (upper right panel), **20** (lower left panel), and **21** (lower right panel) with the active site of DHFR.

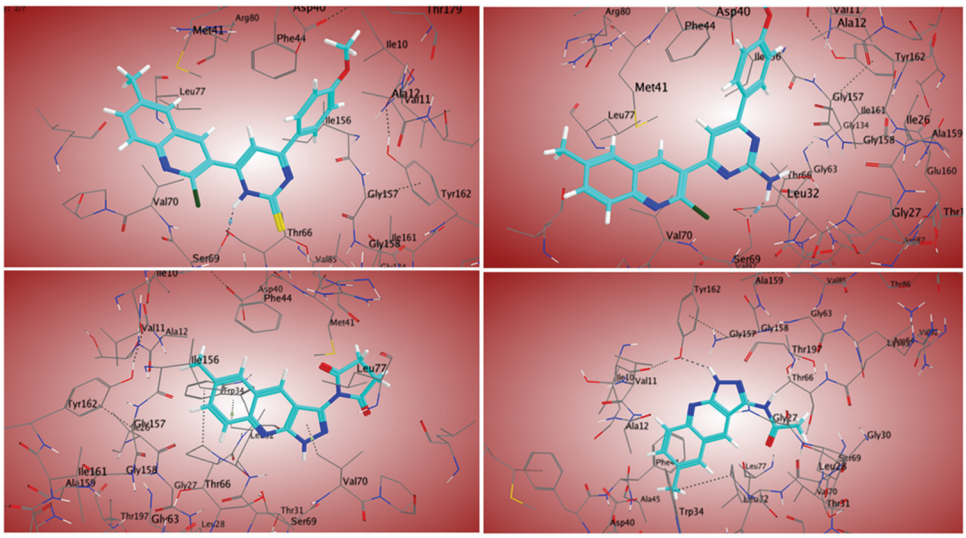

Fig. 8 3D interactions of compounds **15** (upper left panel), **16** (upper right panel), **20** (lower left panel), and **21** (lower right panel) with the active site of DHFR.

rule.[68,69] Lipinski stated that the intestinal absorption of a molecule is more likely to be good enough if it fulfills at least three rules of the following: (i) molecular weight < 500; (ii) number of H bond donors ≤ 5; (iii) number of H bond acceptors ≤ 10; (iv) $\log P < 5$. The bioavailability of medications violating more than one is expected to be not good enough. While the reference antimicrobial drugs gentamicin and amphotericin B violated two or more of Lipinski's rules, all the highest active derivatives in this study (**12**, **15**, **16**, **20**, **21**, and **22**) gratifyingly, satisfied all the Lipinski's rules except compounds **12** and **15**, which are only violating the log *P*. All the new ligands own acceptable numbers of hydrogen bond acceptors (between 3 and 5) and only two or lesser hydrogen bond donor groups. These numbers of HB acceptors and donors in the new compounds agree with Lipinski's rules. Additionally, ADMET profiles of the new quinoline derivatives were tentatively assessed to evaluate their potential to develop new oral drug candidates.

ADMET profiling study was conducted using the pkCSM descriptors algorithm protocol.[70] The absorption of a drug is depending on a number of factors, including intestinal absorption, membrane permeability, skin permeability, and P-glycoprotein substrate or inhibitor. Drug distribution is depending on the volume of distribution (VDss), the blood–brain barrier permeability (logBB), and CNS permeability. Metabolism is predicted depending on the CYP models for a substrate or inhibition. Excretion is predicted based on the total clearance and the renal OCT2 substrate. The toxicity of the

Table 5 ADMET profile of the most active derivatives and reference antimicrobial agents

Parameter	12	15	16	20	21	22	Amp.	Gent.	Amph. B
Molecular properties									
Molecular weight	337.806	393.899	376.847	280.287	240.266	274.711	349.412	477.603	924.091
Log *P*	5.10132	5.99181	4.91142	2.07292	2.37792	2.59682	0.3181	−3.3275	0.7117
Rotatable bonds	4	3	3	1	1	2	4	7	3
HB acceptors	3	4	5	4	3	3	5	12	17
HB donors	0	1	1	1	2	2	3	8	12
Surface area	145.103	166.392	161.373	119.313	103.218	113.521	143.121	194.977	380.536
Absorption									
Water solubility	−5.939	−4.073	−3.926	−3.216	−3.078	−3.169	−2.396	−2.56	−2.937
Intestinal abs. (human)	96.098	91.663	95.785	93.931	94.527	94.192	43.034	13.46	0
Distribution									
VDss (human)	0.176	0.297	0.261	0.369	0.384	0.284	−1.23	−0.967	−0.37
CNS permeability	−1.326	−1.389	−1.748	−2.444	−2.365	−2.417	−3.166	−5.49	−3.718
Metabolism									
CYP3A4 substrate	Yes	Yes	Yes	No	No	No	No	No	No
CYP3A4 inhibitor	No	Yes	Yes	No	No	No	No	No	No
Excretion									
Total clearance	−0.03	0.157	0.127	0.333	0.354	0.27	0.337	0.722	−1.495
Toxicity									
AMES toxicity	No	Yes	Yes	No	Yes	Yes	No	No	No
Max. tolerated dose	0.502	0.392	0.292	0.016	0.298	0.375	0.952	0.694	0.292
hERG I inhibitor	No	No	No	No	No	No	No	No	No
hERG II inhibitor	Yes	Yes	Yes	No	No	No	No	No	No
Oral rat acute toxicity (LD_{50})	2.473	3.089	2.81	2.4	2.39	2.489	1.637	2.016	2.518
Hepatotoxicity	Yes	Yes	Yes	Yes	No	Yes	Yes	No	No
Minnow toxicity	−1.895	−0.971	−1.721	1.513	1.471	1.063	4.232	5.959	11.261

drugs is predicted depending on AMES toxicity, hERG inhibition, hepatotoxicity, and skin sensitization. All of these parameters were calculated for the six highest potent quinoline derivatives as well as to reference marketed antimicrobial agents. After evaluation of ADMET properties (Table 5), we can propose that the new derivatives have the advantage of better intestinal absorption in humans over all reference drugs (91.6–96.1) compared with zero in the case of amphotericin B, and 13.4–43.0 in case of ampicillin and gentamicin. This advantage may be attributed to the superior lipophilicity of the new compounds, which would make them able to go along biological membranes.[71] Therefore, they may have significantly good bioavailability after oral administration.

Studying the CNS permeability, the chalcone derivative **12** displayed the highest ability to penetrate CNS (CNS permeability = −1.32), while reference antimicrobials showed lower abilities to penetrate (CNS permeability ≤ -3.16). As well, it was clear that in contradiction of the three reference drugs, three out of six of the new compounds could inhibit the main cytochrome involved in drug metabolism, cytochrome P3A. This ability may also be attributed to the higher lipophilicity of our constructed quinolines. Excretion was assessed in the term of total clearance, a parameter related to drug bioavailability, and is substantial in deciding dosing intervals. The tabulated results demonstrated that the pyrazoloquinoline derivative **21** and gentamicin revealed the highest total clearance values (0.35 and 0.72, respectively), compared with other ligands, especially chalcone **12**, and standard antifungal, which showed the lowest total clearance value (−0.03 and −1.49, respectively). Thus, **12** is expected to be excreted faster, and consequently needs dosing intervals of shorter duration. Toxicity is the last parameter studied in the ADMET profile of new quinolines. In this regard, one critical drawback of four new quinolines in the present study is the positive probability of AMES toxicity, which means that the new ligands are expected to be mutagenic and hence may act as carcinogens. Additionally, as revealed in Table 5, ampicillin and all the new ligands except **21** are sharing the disadvantage of hepatotoxicity. Gratifyingly, all designed compounds are free from the cardiotoxic probability (no hERG I inhibitory effect) and showed comparable tolerability (0.29–0.50) with that of ampicillin and gentamicin. Finally, the oral acute toxic doses of the new compounds (LD_{50}), are almost higher than those of all marketed reference antimicrobial agents.

3. Conclusion

This study reports the synthesis and *in vitro* antimicrobial evaluation of novel 6-methylquinoline derivatives attached with different pharmacophoric fragments at C-3 as well as novel pyrazolo[3,4-*b*]quinoline derivatives as dual inhibitors of DNA gyrase and DHFR. The preliminary antimicrobial activity of new compounds was assessed against a panel of seven pathogenic bacterial and fungal microbes. Six of the new derivatives (**12**, **15**, **16**, **20**, **21**, and **22**) displayed relatively potent antimicrobial activity with a relative potency range of 80–113%. As well, subsequent docking studies of the most active compounds were conducted to rationalize the binding affinity of new compounds to the active sites of DNA gyrase and *Aspergillus flavus* DHFR enzymes. Overall, this study led us to identify six novel quinolines with interesting antimicrobial activity and DNA gyrase/DHFR inhibitory potentials.

4. Experimental section

4.1. General

Melting points were measured using electrothermal (Stuart SMP30) apparatus and were uncorrected. Infrared spectra were recorded on Pye Unicam SP 1000 IR spectrophotometer at the Pharmaceutical Analytical Unit, Faculty of Pharmacy, Al-Azhar University. ^{1}H NMR and ^{13}C NMR spectra were recorded in DMSO-d_6 at 300 and 100 MHz, respectively, on a Varian Mercury VXR-300 NMR spectrometer at NMR Lab, Faculty of Science, Cairo University. TMS was used as an internal standard, chemical shifts were related to that of the solvent. Chemical shift and coupling constant values are listed in ppm and Hz, respectively. Mass spectra and elemental analyses were carried out at the Regional Center of Mycology and Biotechnology, Al-Azhar University, Cairo, Egypt. Reaction progress was monitored with Merck silica gel IB2-F plates (0.25 mm thickness) and was visualized under a UV lamp using different solvent systems as mobile phases. Reagents and starting *p*-toluidine, phosphorusoxy chloride, *p*-methoxyacetophenone, hydrazine,hydroxylamine, thiourea, guanidine, urea and acid anhydride, and acid halide derivatives were purchased from Aldrich chemical company and were used as received. Compounds **9** and **11** were synthesized according to directions of the previously reported procedures.[23] For preparation of the starting 2-chloro-6-methylquinoline-3-carbaldehyde (**9**), DMF and $POCl_3$ were allowed to react at 0 °C for 2 h, and then *p*-methyl acetanilide was added to the reaction mixture. The overall reactant ratio was found to be a critical issue to obtain the desired product in good yield. Different ratios have been tried and the optimum one was 1 : 3 : 12 (*p*-methylacetanilide:DMF:$POCl_3$). The reaction of the carbonitrile **10** with hydrazine hydrate gave 6-methyl-1*H*-pyrazolo[3,4-*b*]quinolin-3-amine (**11**).

4.2. Synthesis of (*E*)-3-(2-chloro-6-methylquinolin-3-yl)-1-(4-methoxyphenyl)prop-2-en-1-one (12)

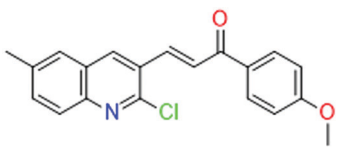

To a stirred and ice-cooled aqueous solution of sodium hydroxide (10 mmol, 50% w/w) and absolute ethanol (15 ml), 4-methoxyacetophenone (1.5 g, 10 mmol) was added followed by 2-chloro-6-methylquinoline-3-carbadehyde (**9**, 2.05 g, 10 mmol).[72] The reaction mixture was vigorously stirred for 3 hours while the temperature was maintained below 25 °C till the reaction mixture became thick. The reaction mixture was left in the refrigerator overnight. The formed precipitate was filtered off under vacuum and washed with copious amounts of water until the filtrates became neutral to litmus paper, washed with three repetitive portions of ice-cold ethanol (20 ml), and then finally recrystallized from ethanol to afford compound **12** as a yellowish white solid. Yield: 80%; m.p. 129–131 °C. IR (KBr) cm^{-1}: 3050 (CH aromatic), 2950 (CH aliphatic), 1655 (C═O). ^{1}H NMR (DMSO-d_6) δ ppm: 9.0 (s, 1H, quinoline-H4), 8.2 (d, 2H, J = 9.0 Hz, phenyl-H2,H6 protons), 8.1 (d, 1H, J = 15.0 Hz, CH alkene β proton), 7.9 (d, 1H, J = 15.0 Hz, CH alkene α proton), 7.8 (d, 1H, J = 9.0 Hz, quinoline-H8), 7.5 (d, 1H, quinoline-H7), 7.4 (s, 1H, quinoline- H5), 7.1 (d, 2H, J = 9.0 Hz, phenyl-H3, H5 protons), 3.8 (s, 3H, phenyl-OCH_3) 2.3 (s, 3H, quinoline-CH_3). ^{13}C NMR (DMSO-d_6, 100 MHz) δ (ppm): 165.5 (C═O), 156.1 (phenyl-C4), 143.4 (quinoline-C2), 145.2 (enone, β carbon), 143.4 (quinoline-C8a), 136.7 (quinoline-C6), 135.6 (quinoline-C4), 135.2 (quinoline-C7), 135.0 (phenyl-C2, C6), 127.6 (quinoline-C3), 127.4 (phenyl-C1), 127.2 (quinoline-C8), 126.4 (enone, α carbon), 123.8 (quinoline-C4a), 119.8 (quinoline-C5), 104.5 (phenyl-C3, C5), 53.8 (OCH_3), 20.9 (CH_3). MS (*m*/*z*): 339 ($C_{20}H_{16}ClNO_2$, 1.7%, M + 2), 337 ($C_{20}H_{16}ClNO_2$, 5%, M^+), 302 ($C_{20}H_{16}NO_2$, 78%), 271 ($C_{19}H_{13}NO$, 3.8%), 256 ($C_{18}H_{10}NO$, 23.7%). Anal. calc. for: ($C_{20}H_{16}ClNO_2$) (M.W. = 337): C, 71.11; H, 4.77; N, 4.15%; found: C, 71.19; H, 4.74; N, 4.21%.

4.3. Synthesis of 2-chloro-3-[3-(4-methoxy-phenyl)-4,5-dihydro-2*H*-pyrazol-5-yl]-6-methyl-quinoline (13)

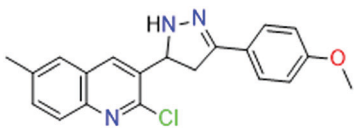

A mixture of chalcone **12** (3.37 g, 10 mmol) and hydrazine hydrate (1 ml, 20 mmol) was stirred in ethanol (20 ml) and heated at reflux for 7 hours. After the reaction was completed, the mixture was concentrated by evaporating the solvent under reduced pressure, and then poured onto ice water. The obtained precipitate was filtered off, washed with water, and recrystallized from ethanol to afford compound **13** as white needles. Yield: 70%; m.p. 116–118 °C. IR (KBr) cm^{-1}: 3290 (NH), 3050 (CH aromatic), 2950 (CH aliphatic). ^{1}H NMR (DMSO-d_6) δ ppm: 8.4 (s, 1H, quinoline-H4), 7.8 (d, 2H, J = 9.0 Hz, phenyl-H2,H6), 7.8 (d, 1H, J = 9.0 Hz, quinoline-H8), 7.6 (s, 1H, NH, D_2O-exchangeable), 7.6 (d, 1H, J = 9.0 Hz, quinoline-H7), 7.5 (s, 1H, quinoline- H5), 6.9 (d, 2H, J = 9.0 Hz, phenyl-H3, H5), 5.1 (t, 1H, J = 15.3 Hz, pyrazole-H5), 3.7 (s, 3H, OCH_3 of phenyl), 3.6 (dd, 1H, J = 16, 9,2 Hz, pyrazole-H4 axial proton), 2.9 (dd, 1H, J = 16.4, 9.2 Hz, pyrazole-H4 equatorial proton) 2.5 (s, 3H, CH_3 of quinoline). ^{13}C NMR (DMSO-d_6, 100 MHz) δ (ppm): 168.4 (phenyl-C4), 158.9 (pyrazole-C3), 155.5 (quinoline-C2), 147.7 (quinoline-C8a), 147.1 (quinoline-C6), 146.2 (quinoline-C4), 143.5 (quinoline-C-7), 136.7 (quinoline-C3), 135.7 (phenyl-C1), 135.3 (phenyl-C2, C6), 133.5 (quinoline-C8), 131.2 (quinoline-C4a), 127.4 (quinoline-C5), 127.1 (phenyl-C3, C5), 61.0 (pyrazole-C5), 60.0 (pyrazole-C4), 42.3 (OCH_3), 20.8 (CH_3). MS (*m*/*z*): 353 ($C_{20}H_{18}ClN_3O$, 9.4%, M + 2), 351 ($C_{20}H_{18}ClN_3O$, 37.11%, M^+), 175 ($C_{10}H_7ClN$, 100%). Anal. calc. for: ($C_{20}H_{18}ClN_3O$) (M.W. = 351): C, 68.28; H, 5.15; N, 11.94%; found: C, 68.31; H, 5.39; N, 11.43%.

4.4. Synthesis of 2-chloro-3-[3-(4-methoxy-phenyl)-4,5-dihydro-isoxazol-5-yl]-6-methyl-quinoline (14)

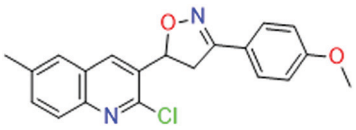

A mixture of chalcone **12** (3.37 g, 10 mmol) and hydroxylamine hydrochloride (0.69 g, 10 mmol) was stirred in ethanol (20 ml), and then sodium hydroxide (0.8 g, 20 mmol) was added. The reaction mixture was heated to reflux for 7 hours, and then the solvent was evaporated under reduced pressure and poured into ice water. The obtained precipitate was filtered off, washed with a copious amount of water, and recrystallized from ethanol to afford the compound **14** as yellowish solid. Yield: 65%; m.p. 130–132 °C. IR (KBr) cm^{-1}: 3050 (CH aromatic), 2950 (CH aliphatic), 1590 (C = N). ^{1}H NMR (DMSO-d_6) δ ppm: 8.3 (s, 1H, quinoline- H4), 7.8 (d, 1H, J = 9.0 Hz, quinoline-H8), 7.6 (d, 2H, J = 9.0 Hz, phenyl-H2, H6), 7.3 (s, 1H, quinoline-H5), 7.4 (d, 1H, J = 9.0 Hz, quinoline- H7), 7.2 (d, 2H, J = 9.0 Hz, phenyl-H3,H5), 5.7 (t, 1H, J = 14 Hz, isoxazole-H5), 4.0 (dd, 1H, J = 11, 5 Hz, isoxazole-H4 axial proton), 3.7 (s, 3H, phenyl OCH_3), 3.6 (dd, 1H, J = 17, 4.8 Hz, isoxazole-H4 equatorial proton) 2.4 (s, 3H, quinoline CH_3). ^{13}C NMR (DMSO-d_6, 100 MHz) δ (ppm): 163.1 (phenyl-C4), 160.8 (isoxazole-C3), 138.3 (quinoline-C2), 136.4 (quinoline-C8a), 133.0 (quinoline-C6), 131.3 (quinoline-C4), 130.6 (quinoline-C-7), 130.5 (quinoline-C3), 127.9 (phenyl-C1), 125.3 (phenyl-C2, C6), 123.8 (quinoline-C8), 119.0 (quinoline-C4a), 115.0 (quinoline-C5), 114.1 (phenyl-C3, C5), 77.9 (isoxazole-C5), 55.5 (OCH_3), 42.2 (isoxazole-C4), 20.3 (CH_3). MS (m/z): 354 ($C_{20}H_{17}ClN_2O_2$, 0.5%, M + 2), 352 ($C_{20}H_{17}ClN_2O_2$, 1.73%, M^+), 317 ($C_{20}H_{17}N_2O_2$, 35.77%), 185($C_{12}H_{11}NO$, 12.17%)). Anal. calc. for: ($C_{20}H_{17}ClN_2O_2$) (M.W. = 352): C, 68.09; H, 4.86; N, 7.94%; found: C, 68.13; H, 4.97; N, 7.87%.

4.5. Synthesis of 6-(2-Chloro-6-methyl-quinolin-3-yl)-4-(4-methoxy-phenyl)-1*H*-pyrimidine-2-thione (15)

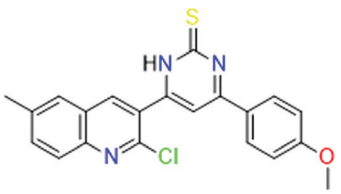

A mixture of chalcone **12** (3.37 g, 10 mmol) and thiourea (0.76 g, 10 mmol) was stirred in ethanol (20 ml) and then sodium hydroxide (0.8 g, 20 mmol) was added to it. The mixture was heated at reflux for 7 hours. After the reaction was completed the solvent was concentrated by evaporation under reduced pressure and poured into ice water. The obtained precipitate was filtered, washed with water, and recrystallized from ethanol to give the titled compound as a dark yellow solid. Yield: 40%; m.p. 140–142 °C. IR (KBr) cm^{-1}: 3290 (NH), 3050 (CH aromatic), 2950 (CH aliphatic). ^{1}HNMR (DMSO-d_6) δ ppm: 11.9 (s, 1H, NH, D_2O-exchangeable proton), 8.5 (s, 1H, quinoline-H4), 8.3 (d, 1H, J = 15 Hz, quinoline-H8), 8 (d, 2H, J = 9.0 Hz, phenyl-H2,H6), 7.7 (d, 1H, J = 15 Hz, quinoline-H7), 7.3 (s, 1H, quinoline-H5), 7.2 (s, 1H, pyrimidine-H5), 7.1 (d, 2H, J = 9.0 Hz, phenyl-H3,H5), 3.8 (s, 3H, phenyl OCH_3) 2.36 (s, 3H, quinoline CH_3. ^{13}C NMR (DMSO-d_6, 100 MHz) δ (ppm): ^{13}C NMR (DMSO-d_6, 100 MHz) δ (ppm): 187.7 (C = S), 187.7 (pyrimidine-C6), 163.1 (pyrimidine-C4), 160.8 (phenyl-C4), 140.9 (quinoline-C2), 138.3 (quinoline-C8a), 136.9 (quinoline-C6), 133.0 (quinoline-C4), 131.3 (quinoline-C-7), 130.6 (quinoline-C3), 130.5 (phenyl-C2, C6), 127.9 (quinoline-C8), 125.9 (quinoline-C4a, C5), 123.8 (quinoline-C5), 119.0 (phenyl-C1), 115.0 (phenyl-C3, C5), 114.1 (pyrimidine-C5), 55.5 (OCH_3), 20.3 (CH_3). MS (m/z): 395 ($C_{21}H_{16}ClN_3OS$, 0.15%, M + 2), 393 ($C_{21}H_{16}ClN_3OS$, 0.99%, M^+), 200 ($C_{12}H_7ClN$, 100%), 175 ($C_{10}H_6ClN$). Anal. calc. for: ($C_{21}H_{16}ClN_3O$ S) (M.W. = 393): C, 64.03; H, 4.09; N, 10.67%; found: C, 64.12; H, 4.16; N, 10.78%.

4.6. Synthesis of 4-(2-chloro-6-methyl-quinolin-3-yl)-6-(4-methoxy-phenyl)-pyrimidin-2-ylamine (16)

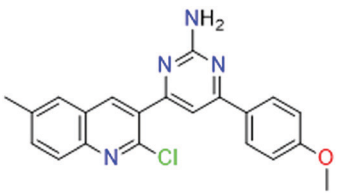

A mixture of chalcone **12** (3.37 g, 10 mmol) and guanidine hydrochloride (0.95 g, 10 mmol) was stirred in absolute ethanol (20 ml), and then sodium hydroxide (0.8 g, 20 mmol) was added. The reaction mixture was heated at reflux for 7 hours. After completion of the reaction, as detected by TLC, the solvent was concentrated under reduced pressure, and then poured into ice water (50 ml). The obtained solid was filtered off, washed and recrystallized from ethanol to afford the desired compound as yellow solid. Yield: 60%; m.p. 190–192 °C. IR (KBr) cm^{-1}: 3300 (NH_2), 3050 (CH aromatic), 2950 (CH aliphatic). ^{1}H NMR (DMSO-d_6) δ ppm: 8.6 (s, 1H, quinoline-H4), 8.1 (d, 2H, J = 9.0 Hz, phenyl-H2,H6), 7.9 (d, 1H, J = 9.0 Hz, quinoline-H8), 7.7 (s, 1H, pyrimidine-H5), 7.5 (d, 1H, J = 9.0 Hz, quinoline-H7), 7.4 (s, 1H, quinoline-H5), 7.0 (d, 2H, J = 9.0 Hz, phenyl-H3, H5), 6.6 (s, 2H, NH_2, D_2O-exchangeable protons), 3.8 (s, 3H, phenyl OCH_3), 2.4 (s, 3H, quinoline CH_3). ^{13}C NMR (DMSO-d_6, 100 MHz) δ (ppm): 187.7 (C═O), 187.7 (pyrimidine-C6), 163.1 (pyrimidine-C4), 160.8 (phenyl-C4), 140.9 (quinoline-C2), 138.3 (quinoline-C8a), 136.9 (quinoline-C6), 133.0 (quinoline-C4), 131.3 (quinoline-C-7), 130.6 (quinoline-C3), 130.5 (phenyl-C2, C6), 127.9 (quinoline-C8), 125.9 (quinoline-C4a, C5), 123.8 (quinoline-C5), 119.0 (phenyl-C1), 115.0 (phenyl-C3, C5), 114.1 (pyrimidine-C5), 55.5 (OCH_3), 20.3 (CH_3). MS (m/z): 378 ($C_{21}H_{17}ClN_4O$, 27.34%, M + 2), 376 ($C_{21}H_{17}ClN_4O$, 70.33%, M^+), 342 ($C_{21}H_{17}N_4O$, 100%). Anal. calc. for: ($C_{21}H_{17}ClN_4O$) (M.W. = 376): C, 66.93; H, 4.55; N, 14.87%; found: C, 66.8; H, 4.47; N, 14.75%.

4.7. Synthesis of 6-(2-chloro-6-methyl-quinolin-3-yl)-4-(4-methoxy-phenyl)-1*H*-pyrimidin-2-one (17)

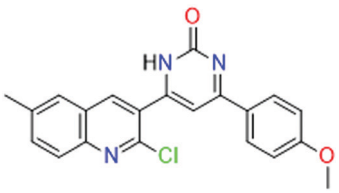

A mixture of chalcone **12** (3.37 g, 10 mmol) and urea (0.6 g, 10 mmol) was stirred in ethanol (20 ml), and then hydrochloric acid (2 ml) was added. The mixture was heated at reflux for 7 hours. After completion of the reaction, the solvent was concentrated under reduced pressure and poured into ice water (50 ml). The obtained precipitate was filtered off, washed with distilled water, and finally recrystallized from ethanol to yield the titled compound as a yellowish white solid. Yield: 60%; m.p. 178–180 °C. IR (KBr) cm^{-1}: 3290 (NH), 3050 (CH aromatic), 2950 (CH aliphatic) 1679 (C═O). ^{1}H NMR (DMSO-d_6) δ ppm: 11.98 (s, 1H, NH, D_2O-exchangeable proton), 8.5 (s, 1H, quinoline-H4), 8.3 (d, 1H, J = 15 Hz, quinoline-H8), 8.0 (d, 2H, J = 9.0 Hz, phenyl-H2,H6), 7.7 (d, 1H, J = 15 Hz, quinoline-H7), 7.3 (s, 1H, quinoline-H5), 7.2 (s, 1H, pyrimidine-H5), 7.1 (d, 2H, J = 9.0 Hz, phenyl-H3,H5), 3.8 (s, 3H, phenyl OCH_3) 2.4 (s, 3H, quinoline CH_3). ^{13}C NMR (DMSO-d_6, 100 MHz) δ (ppm): 164.6 (pyrimidine-C4), 163.4 (pyrimidine-C6), 157.6 (C═O), 163.1 (phenyl-C4), 160.8 (quinoline-C2), 149.6 (quinoline-C3), 138.4 (quinoline-C8a), 136.9 (quinoline-C6), 133.0 (quinoline-C4), 131.3 (quinoline-C-7), 130.5 (phenyl-C1), 127.9 (phenyl-C2, C6), 125.9 (quinoline-C8), 123.8 (quinoline-C4a), 119.0 (quinoline-C5), 115.0 (phenyl-C3, C5), 114.1 (pyrimidine-C5), 55.5 (OCH_3), 20.2 (CH_3). MS (m/z): 379 ($C_{21}H_{16}ClN_3O_2$, 2.72%, M + 2), 377 ($C_{21}H_{16}ClN_3O_2$, 4%, M^+), 346 ($C_{20}H_{13}ClN_3O$, 6.76%), 270 ($C_{14}H_9ClN_3O$, 12.14%), 216 ($C_{12}H_9ClN_2$, 5.68%), 92 (C_7H_8, 100%). Anal. calc. for: ($C_{21}H_{16}ClN_3O_2$) (M.W. = 377): C, 66.76; H, 4.27; N, 11.12%; found: C, 66.84; H, 4.33; N, 11.21.

4.8. General procedures for the synthesis of pyrazolo[3,4-*b*] quinoline derivatives 18–22

A mixture of 6-methyl-1*H*-pyrazolo[3,4-*b*]quinolin-3-amine (**11**, 1.98 g, 10 mmol) and the appropriate acid anhydride or acid halide derivatives (10 mmol) in acetic acid (50 ml) was heat to reflux for 1–4 hours (Scheme 1).[23] After completing the reaction, as observed by TLC, the reaction mixture was filtered off while hot, and the solvent was concentrated, the separated solid was filtered and recrystallized from ethanol to afford the target final product.

4.8.1. 2-(6-Methyl-1*H*-pyrazolo[3,4-*b*]quinolin-3-yl) isoindoline-1,3-dione (18)

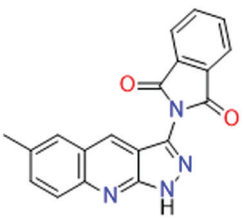

Faint brown solid. Yield: 70%; m.p. 290–292 °C. IR (KBr) cm^{-1}: 3426 (N–H), 3015 (C–H aromatic), 2892 (C–H aliphatic), 1645 (C═O). ^{1}H NMR (DMSO-d_6) δ ppm: 13.8 (s, 1H, NH, D_2O-exchangeable), 8.8 (s, 1H, quinoline-H4), 8–7.9 (m, 5H, Ar H's), 7.8 (s, 1H, quinoline-H5), 7.6 (d, 1H, J = 9.0 Hz, quinoline-H7), 2.1 (s, 3H, CH_3). ^{13}C NMR (DMSO-d_6, 100 MHz) δ (ppm): 166.9 (C═O), 151.3 (pyrazole-C3), 136.7 (quinoline-C2), 135.6 (quinoline-C8a), 134.2 (quinoline-C4), 133.8 (quinoline-C6), 133.0 (isoindole-C5, C6), 132.0 (isoindole-C4a, C7a), 130.0 (quinoline-C7), 129.2 (quinoline-C-8), 128.1 (quinoline-C5), 127.6 (isoindole-C4, C7), 125.2 (quinoline-C4a), 112.1 (quinoline-C3), 21.4 (CH_3). MS (m/z): 328 ($C_{19}H_{12}N_4O_2$, 65.41%, M^+), 182 ($C_{11}H_8N_3$, 5%), 167 ($C_{10}H_5N_3$, 2.9%), 141 ($C_9H_5N_2$, 4.78%), 126 (C_9H_4N, 1.7%). Anal. calc. for: ($C_{19}H_{12}N_4O_2$) (M.W. = 328): C, 69.51; H, 3.68; N, 17.06; found: C, 69.60; H, 3.73; N, 17.28%.

4.8.2. 1-(6-Methyl-1*H*-pyrazolo[3,4-*b*]quinolin-3-yl)-1*H*-pyrrole-2,5-dione (19)

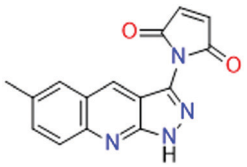

Faint brown solid. Yield: 65%; m.p. 230–232 °C. IR (KBr) cm^{-1}: 3229 (N–H), 3051 (C–H aromatic), 2994 (C–H aliphatic), 1683 (C═O). ^{1}H NMR (DMSO-d_6) δ ppm: 13.9 (s, 1H, NH), 8.9 (s, 1H, quinoline-H4), 7.8 (s, 2H, pyrrole-H's), 7.6 (d, 1H, J = 9.0 Hz, quinoline-H8), 7.5 (d, 1H, J = 9.0 Hz, quinoline-H7), 6.9 (s, 1H, quinoline-H5), 2.1 (s, 3H, CH_3). ^{13}C NMR (DMSO-d_6, 100 MHz) δ (ppm): 168.9 (C═O), 151.9 (pyrazole-C3), 147.1 (quinoline-C2), 140.5 (quinoline-C8a), 133.7 (quinoline-C4), 133.0 (quinoline-C6), 132.7 (pyrrolidinedione-C3, C4), 128.4 (quinoline-C7), 127.4 (quinoline-C8), 123.8 (quinoline-C5), 110.4 (quinoline-C4a), 22.9 (CH_3). MS (m/z): 278 ($C_{15}H_{10}N_4O_2$, 1.27%, M^+), 198 ($C_{11}H_{10}N_4$, 100%), 182 ($C_{11}H_8N_3$, 5.24%), 167 ($C_{10}H_5N_3$, 8.9%), 141 ($C_9H_5N_2$, 8.9%). Anal. calc. for: ($C_{15}H_{10}N_4O_2$) (M.W. = 278): C, 64.74; H, 3.62; N, 20.13; found: C, 64.81; H, 3.62; N, 20.15%.

4.8.3. 1-(6-Methyl-1*H*-pyrazolo[3,4-*b*]quinolin-3-yl) pyrrolidine-2,5-dione (20)

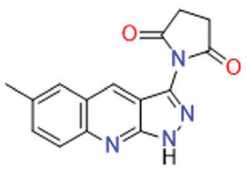

Reddish white solid. Yield: 60%; m.p. 260–262 °C. IR (KBr) cm^{-1}: 3265 (N–H), 3077 (C–H aromatic), 2918 (C–H aliphatic), 1664 (C═O). ^{1}H NMR (DMSO-d_6) δ ppm: 10.8 (s, 1H, NH), 8.9 (s, 1H, quinoline-H4), 7.8 (d, 1H, J = 9.0 Hz, quinoline-H8), 7.6 (d, 1H, J = 9.0 Hz, quinoline-H7), 7.5 (s, 1H, quinoline-H5), 2.9 (s, 4H, $2CH_2$), 2.2 (s, 3H, CH_3). ^{13}C NMR (DMSO-d_6, 100 MHz) δ (ppm): 177.1 (C═O), 169.0 (pyrazole-C3), 152.0 (quinoline-C2), 147.1 (quinoline-C8a), 140.5 (quinoline-C4), 133.7 (quinoline-C6), 132.9 (quinoline- C7), 132.7 (quinoline-C8), 128.4 (quinoline-C-5),

127.6 (quinoline-C4a), 123.8 (quinoline-C3), 29.32 (pyrrolidinedione-C3, C4), 21.4 (CH_3). MS (*m*/*z*): 280 ($C_{15}H_{12}N_4O_2$, 5.7%, M^+), 198 ($C_{11}H_{10}N_4$, 100%), 182 ($C_{11}H_8N_3$, 2.58%), 167 ($C_{10}H_5N_3$, 4.15%), 141 ($C_9H_5N_2$, 3.97%). Anal. calc. for: ($C_{15}H_{12}N_4O_2$) (M.W. = 280): C, 64.28; H, 4.32; N, 19.99; found: C, 64.32; H, 4.38; N, 20.02%.

4.8.4. *N*-(6-Methyl-1*H*-pyrazolo[3,4-*b*]quinolin-3-yl)-acetamide (21)

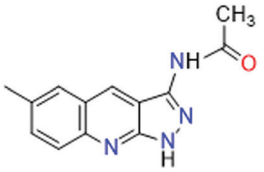

Yellowish-white solid. Yield: 78%; m.p. 230–232 °C. IR (KBr) cm^{-1}: 3214 (N–H), 3077 (C–H aromatic), 2990 (C–H aliphatic), 1675 (C═O). ^{1}H NMR (DMSO-d_6) δ ppm: 10.8 (s, 1H, NH), 9.04 (s, 1H, NHCO), 8.9 (s, 1H, quinoline-H4), 7.8 (d, 1H, J = 9.0 Hz, quinoline-H8), 7.6 (d, 1H, J = 9.0 Hz, quinoline-H7), 7.4 (s, 1H, quinoline-H5), 2.2 (s, 3H, quinoline-CH_3), 1.8 (s, 3H, CH_3). ^{13}C NMR (DMSO-d_6, 100 MHz) δ (ppm): 161.8 (C═O), 149.4 (pyrazole-C3), 148.9 (quinoline-C2), 141.2 (quinoline-C8a), 136.4 (quinoline-C4), 133.0 (quinoline-C6), 129.7 (quinoline-C7), 128.4 (quinoline-C8), 127.3 (quinoline-C5), 125.3 (quinoline-C4a), 121.1 (quinoline-C3), 23.4 (CH_3), 21.0 (CH_3). MS (*m*/*z*): 240 ($C_{13}H_{12}N_4O$, 42.17%, M^+), 225 ($C_{12}H_9N_4O$, 100%). Anal. calc. for: ($C_{13}H_{12}N_4O$) (M.W. = 240): C, 64.99; H, 5.03; N, 23.32; found: C, 65.12; H, 5.01; N, 23.41%.

4.8.5. 2-Chloro-*N*-(6-methyl-1*H*-pyrazolo[3,4-*b*]quinolin-3-yl)-acetamide (22)

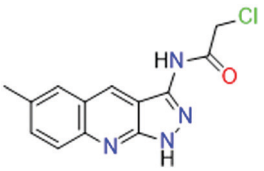

Yellowish-white solid. Yield: 93%; m.p. 270–272 °C. IR (KBr) cm^{-1}: 3224 (N–H), 3035 (C–H aromatic), 2995 (C–H aliphatic), 1669 (C═O). ^{1}H NMR (DMSO-d_6) δ ppm: 13.1 (s, 1H, NH), 11.2 (s, 1H, NHCO), 8.9 (s, 1H, quinoline-H4), 7.8 (d, 1H, J = 9.0 Hz, quinoline-H8), 7.6 (d, 1H, J = 9.0 Hz, quinoline-H7), 7.61 (s, 1H, quinoline-H5), 4.4 (s, 2H, CH_2), 2.48 (s, 3H, CH_3). ^{13}C NMR (DMSO-d_6, 100 MHz) δ (ppm): 165.5 (C═O), 139.9 (pyrazole-C3), 139.5 (quinoline-C2), 137.4 (quinoline-C8a), 134.2 (quinoline-C4), 133.4 (quinoline-C6), 133.2 (quinoline-C7), 130.1 (quinoline-C8), 128.5 (quinoline-C5), 127.0 (quinoline-C4a), 123.8 (quinoline-C3), 43.6 (CH_2), 20.8 (CH_3). MS (*m*/*z*): 276 ($C_{13}H_{11}Cl\ N_4O$, 2.72%, M + 2), 274 ($C_{13}H_{11}ClN_4O$, 7.76%, M^+), 225 ($C_{12}H_9N_4O$, 9.86%), 198 ($C_{11}H_9N_4$, 100%), 182 ($C_{10}H_6N_4$, 3.52%). Anal. calc. for: ($C_{13}H_{11}ClN_4O$) (M.W. = 274): C, 56.84; H, 4.04; N, 20.40; found: C, 56.92; H, 4.03; N, 20.53%.

4.9. *In vitro* antimicrobial evaluation

Agar-diffusion method[56] was used for the determination of antibacterial and antifungal activity following the directions of Clinical and Laboratory Standards Institute.[56] Briefly, suspensions of the selected microorganisms were uniformly spread using sterile cotton swabs on sterile Petri dishes of nutrient agar for bacteria and Sabouraud agar for fungi. For bacterial strains, suspensions of the microorganisms were prepared by inoculating fresh stock cultures into separate broth tubes, each containing 7 mL of nutrient agar. The inoculated tubes were incubated at 37 °C for 24 hours. Compounds to be tested were prepared in the required concentrations (1 mg in 1 ml DMSO), ampicillin and gentamicin were prepared in the same manner. Nutrient agar was dissolved and distributed in 25 ml quantities in 100 ml conical flasks and was sterilized in an autoclave at 121 °C for 20 minutes. The medium was poured in Petri dishes and allowed to set for 30 minutes at room temperature. Cultures of bacterial strain were spread with dry sterile swabs on the surface of the previously prepared plates. Cups of 6 mm diameters at equal distances were aseptically punched in each plate, one cup was used for the control (DMSO) and two other cups for the standards (Ampicillin, Gentamicin) where the remaining cups were used for the tested compound. The plates were incubated at 37 °C for 24 h then the plates were examined for inhibition zones.

For fungal strains, suspensions of the fungi were prepared by inoculating fresh stock cultures into tubes containing Sabouraud agar. The inoculated tubes were incubated at 25 °C for 48 h. Sabouraud agar was dissolved and distributed in 25 ml quantities in 100 ml conical flasks and was sterilized in an autoclave at 121 °C for 20 minutes. Afterward, the medium was poured into Petri dishes and allowed to set for 30 minutes at room temperature. Cultures of each organism were aseptically spread on the surface of the previously prepared Petri dishes using a dry sterile swab. Cups of 6 mm diameters at equal distances (20 mm) were made on each plate. In each plate, one cup was used to introduce 75 μL of the control and another one for Amphotericin B, while the other cups were used to introduce equal volumes of compounds to be tested. The plates were incubated at 25 °C for 48 h then were examined to measure the inhibition zones.

4.9.1. Determination of the inhibition zones. 75 μL solution of each test compound (1 mg ml^{-1} in DMSO), was placed in a 6 mm-diameter cup in agar plate seeded with the appropriate test pathogen in triplicate. Ampicillin, gentamicin, and amphotericin B (1 mg ml^{-1} in DMSO each) were used as standards for Gram-positive, Gram-negative antibacterial, and antifungal agents, respectively. DMSO as a negative control showed no inhibition zone (IZ). Plates were incubated at 37 °C for 24 h (for bacteria) or at 25 °C for 48 h (for fungi).

4.9.2. Docking studies. Molecular docking experiments were conducted by MOE builder within the Molecular Operating Environment (MOE) software suite (MOE2014, https://www.chemcomp.com/Products.htm) to evaluate the binding free energy and to discover the binding modes toward DNA gyrase and DHFR enzymes (PDB IDs: 4DUH, Resolution: 1.50 Å, https://www.rcsb.org/structure/4DUH; 6DTC: Resolution: 2.00 Å, https://www.rcsb.org/structure/6DTC) and considered as a target for docking simulation.[65,66] Molecular docking

studies were conducted following our previously reported procedures.[73–76]

Author contributions

K. El-Gamal, and H. S. Abulkhair were responsible for the conception and rational design of the work. M. El-Shershaby, M. Alswah and A. Bayoumi were responsible for the data collection and synthesis of new compounds. K. El-Adl, A. Al-Karmalawi, and H. Ahmed, performed the molecular docking study. K. El-Gamal, and H. S. Abulkhair were responsible for analyzing the spectral data. K. El-Adl and H. Abulkhair performed the pharmacokinetic study. All authors contributed to the writing and revision of the manuscript.

Conflicts of interest

The authors declare that there is no conflict of interest.

Acknowledgements

The authors would like to thank the website of https://www.dreamstime.com/ for providing free clipart tools that have been used to design the graphical abstract.

References

1 J. Hyde, C. Gorham, D. E. Brackney and B. Steven, *PLoS One*, 2019, **14**, e0218907, DOI: 10.1371/journal.pone.0218907.
2 W. C. Reygaert, *AIMS Microbiol.*, 2018, **4**, 482–501, DOI: 10.3934/microbiol.2018.3.482.
3 The World Health Organization, Antimicrobial resistance, https://www.who.int/news-room/fact-sheets/detail/antimicrobial-resistance, (accessed 27 April 2021).
4 P. Loomba, J. Taneja and B. Mishra, *J. Global Infect. Dis.*, 2010, **2**, 275, DOI: 10.4103/0974-777X.68535.
5 A. K. McClendon and N. Osheroff, *Mutat. Res., Fundam. Mol. Mech. Mutagen.*, 2007, **623**, 83–97, DOI: 10.1016/j.mrfmmm.2007.06.009.
6 O. H. Rizk, M. G. Bekhit, A. A. B. Hazzaa, E. M. El-Khawass and I. A. Abdelwahab, *Arch. Pharm.*, 2019, **352**, 1900086, DOI: 10.1002/ardp.201900086.
7 A. M. Omar, M. Alswah, H. E. A. Ahmed, A. H. Bayoumi, K. M. El-Gamal, A. El-Morsy, A. Ghiaty, T. H. Afifi, F. F. Sherbiny, A. S. Mohammed and B. A. Mansour, *Bioorg. Chem.*, 2020, **96**, 103656, DOI: 10.1016/j.bioorg.2020.103656.
8 D. C. Hooper and G. A. Jacoby, *Cold Spring Harbor Perspect. Med.*, 2016, **6**, a025320, DOI: 10.1101/cshperspect.a025320.
9 T. D. M. Pham, Z. M. Ziora and M. A. T. Blaskovich, *MedChemComm*, 2019, **10**, 1719–1739, DOI: 10.1039/C9MD00120D.
10 C. MacDougall, B. J. Guglielmo, J. Maselli and R. Gonzales, *Emerging Infect. Dis.*, 2005, **11**, 380–384, DOI: 10.3201/eid1103.040819.
11 P. Cottagnoud and M. G. Täuber, *Curr. Infect. Dis. Rep.*, 2003, **5**, 329–336, DOI: 10.1007/s11908-003-0011-0.
12 B. D. Bax, P. F. Chan, D. S. Eggleston, A. Fosberry, D. R. Gentry, F. Gorrec, I. Giordano, M. M. Hann, A. Hennessy, M. Hibbs, J. Huang, E. Jones, J. Jones, K. K. Brown, C. J. Lewis, E. W. May, M. R. Saunders, O. Singh, C. E. Spitzfaden, C. Shen, A. Shillings, A. J. Theobald, A. Wohlkonig, N. D. Pearson and M. N. Gwynn, *Nature*, 2010, **466**, 935–940, DOI: 10.1038/nature09197.
13 K. Douadi, S. Chafaa, T. Douadi, M. Al-Noaimi and I. Kaabi, *J. Mol. Struct.*, 2020, **1217**, 128305, DOI: 10.1016/j.molstruc.2020.128305.
14 S. Ghosh, S. Pal, K. S. S. Praveena and J. Mareddy, *J. Mol. Struct.*, 2020, **1212**, 128137, DOI: 10.1016/j.molstruc.2020.128137.
15 Centers for Disease Control and Prevention, Antifungal Resistance, https://www.cdc.gov/fungal/antifungal-resistance.html, (accessed 11 May 2021).
16 C. DeJarnette, A. Luna-Tapia, L. R. Estredge and G. E. Palmer, *mSphere*, 2020, **5**(3), e00374–20, DOI: 10.1128/mSphere.00374-20.
17 M. F. El Shehry, M. M. Ghorab, S. Y. Abbas, E. A. Fayed, S. A. Shedid and Y. A. Ammar, *Eur. J. Med. Chem.*, 2018, **143**, 1463–1473, DOI: 10.1016/j.ejmech.2017.10.046.
18 M. H. El-Shershaby, K. M. El-Gamal, A. H. Bayoumi, K. El-Adl, H. E. A. Ahmed and H. S. Abulkhair, *Arch. Pharm.*, 2021, **354**(2), e2000277, DOI: 10.1002/ardp.202000277.
19 N. C. Desai, B. Y. Patel and B. P. Dave, *Med. Chem. Res.*, 2017, **26**, 109–119, DOI: 10.1007/s00044-016-1732-6.
20 P. Nickel and E. Fink, *Arch. Pharm.*, 1972, **305**, 442–448, DOI: 10.1002/ardp.19723050607.
21 S. Bawa, S. Kumar, S. Drabu and R. Kumar, *J. Pharm. Bioallied Sci.*, 2010, **2**, 64, DOI: 10.4103/0975-7406.67002.
22 S. Mirzaei, F. Hadizadeh, F. Eisvand, F. Mosaffa and R. Ghodsi, *J. Mol. Struct.*, 2020, **1202**, 127310, DOI: 10.1016/j.molstruc.2019.127310.
23 E. E. Nasr, A. S. Mostafa, M. A. A. El-Sayed and M. A. M. Massoud, *Arch. Pharm.*, 2019, **352**, 1800355, DOI: 10.1002/ardp.201800355.
24 K. El-Adl, A. G. A. El-Helby, H. Sakr, R. R. Ayyad, H. A. Mahdy, M. Nasser, H. S. Abulkhair and S. S. A. El-Hddad, *Arch. Pharm.*, 2021, **354**(2), 2000279, DOI: 10.1002/ardp.202000279.
25 C. Dong, W. Gao, X. Li, S. Sun, J. Huo, Y. Wang, D. Ren, J. Zhang and L. Chen, *Mol. Diversity*, 2020, DOI: 10.1007/s11030-020-10127-w.
26 M.-J. Chu, W. Wang, Z.-L. Ren, H. Liu, X. Cheng, K. Mo, L. Wang, F. Tang and X.-H. Lv, *Molecules*, 2019, **24**, 1311, DOI: 10.3390/molecules24071311.
27 G. Kumar, V. Siva Krishna, D. Sriram and S. M. Jachak, *Arch. Pharm.*, 2020, **353**, 2000077, DOI: 10.1002/ardp.202000077.
28 O. S. Trefzger, N. V. Barbosa, R. L. Scapolatempo, A. R. Neves, M. L. F. S. Ortale, D. B. Carvalho, A. M. Honorato, M. R. Fragoso, C. Y. K. Shuiguemoto, R. T. Perdomo, M. F. C. Matos, M. R. Chang, C. C. P. Arruda and A. C. M. Baroni, *Arch. Pharm.*, 2020, **353**, 1900241, DOI: 10.1002/ardp.201900241.

29 G. S. Basarab, P. Brassil, P. Doig, V. Galullo, H. B. Haimes, G. Kern, A. Kutschke, J. McNulty, V. J. A. Schuck, G. Stone and M. Gowravaram, *J. Med. Chem.*, 2014, **57**, 9078–9095, DOI: 10.1021/jm501174m.
30 M. H. Hannoun, M. Hagras, A. Kotb, A. A. M. M. El-Attar and H. S. Abulkhair, *Bioorg. Chem.*, 2020, **94**, 103364, DOI: 10.1016/j.bioorg.2019.103364.
31 S. Narwal, S. Kumar and P. K. Verma, *Chem. Cent. J.*, 2017, **11**, 52, DOI: 10.1186/s13065-017-0284-2.
32 M. A. Ismail, S. Al-Shihry, R. K. Arafa and U. El-Ayaan, *J. Enzyme Inhib. Med. Chem.*, 2013, **28**, 530–538, DOI: 10.3109/14756366.2011.654113.
33 B. D. Bax, G. Murshudov, A. Maxwell and T. Germe, *J. Mol. Biol.*, 2019, **431**, 3427–3449, DOI: 10.1016/j.jmb.2019.07.008.
34 M.-J. Chu, W. Wang, Z.-L. Ren, H. Liu, X. Cheng, K. Mo, L. Wang, F. Tang and X.-H. Lv, *Molecules*, 2019, **24**, 1311, DOI: 10.3390/molecules24071311.
35 S. Ihmaid, H. E. A. Ahmed, A. Al-Sheikh Ali, Y. E. Sherif, H. M. Sherif, S. M. Riyadh, M. F. Zayed, H. S. Abulkhair and H. S. Rateb, *Bioorg. Chem.*, 2017, **72**, 234–247, DOI: 10.1016/j.bioorg.2017.04.014.
36 M. I. Abdullah, A. Mahmood, M. Madni, S. Masood and M. Kashif, *Bioorg. Chem.*, 2014, **54**, 31–37, DOI: 10.1016/j.bioorg.2014.03.006.
37 M. Mellado, L. Espinoza, A. Madrid, J. Mella, E. Chávez-Weisser, K. Diaz and M. Cuellar, *Mol. Diversity*, 2020, **24**, 603–615, DOI: 10.1007/s11030-019-09967-y.
38 O. Dror, D. Schneidman-Duhovny, Y. Inbar, R. Nussinov and H. J. Wolfson, *J. Chem. Inf. Model.*, 2009, **49**, 2333–2343, DOI: 10.1021/ci900263d.
39 H. S. Abulkhair, A. Turky, A. Ghiaty, H. E. A. Ahmed and A. H. Bayoumi, *Bioorg. Chem.*, 2020, **100**, 103899, DOI: 10.1016/j.bioorg.2020.103899.
40 H. Abul-Khair, S. Elmeligie, A. Bayoumi, A. Ghiaty, A. El-Morsy and M. H. Hassan, *J. Heterocycl. Chem.*, 2013, **50**, 1202–1208, DOI: 10.1002/jhet.714.
41 A. M. Omar, S. Ihmaid, E.-S. E. Habib, S. S. Althagfan, S. Ahmed, H. S. Abulkhair and H. E. A. Ahmed, *Bioorg. Chem.*, 2020, **99**, 103781, DOI: 10.1016/j.bioorg.2020.103781.
42 F. Chevreuil, A. Landreau, D. Séraphin, G. Larcher, S. Mallet, J.-P. Bouchara and P. Richomme, *J. Enzyme Inhib. Med. Chem.*, 2007, **22**, 563–569, DOI: 10.1080/14756360701425279.
43 M. S. Mohamed, S. M. Awad and A. I. Sayed, *Molecules*, 2010, **15**, 1882–1890, DOI: 10.3390/molecules15031882.
44 M. P. Reddy and G. S. K. Rao, *J. Org. Chem.*, 1981, **46**, 5371–5373, DOI: 10.1021/jo00339a023.
45 S. T. Chill and R. C. Mebane, *Synth. Commun.*, 2009, **39**, 3601–3606, DOI: 10.1080/00397910902788174.
46 M. H. El-Shershaby, A. Ghiaty, A. H. Bayoumi, H. E. A. Ahmed, M. S. El-Zoghbi, K. El-Adl and H. S. Abulkhair, *New J. Chem.*, 2021, **45**, 11136–11152, DOI: 10.1039/d1nj00710f.
47 A. Turky, F. F. Sherbiny, A. H. Bayoumi, H. E. A. Ahmed and H. S. Abulkhair, *Arch. Pharm.*, 2020, **353**(12), 2000170, DOI: 10.1002/ardp.202000170.
48 K. El-Adl, H. M. Sakr, R. G. Yousef, A. B. M. Mehany, A. M. Metwaly, M. A. Elhendawy, M. M. Radwan, M. A. ElSohly, H. S. Abulkhair and I. H. Eissa, *Bioorg. Chem.*, 2021, 105105, DOI: 10.1016/j.bioorg.2021.105105.
49 H. G. Ezzat, A. H. Bayoumi, F. F. Sherbiny, A. M. El-Morsy, A. Ghiaty, M. Alswah and H. S. Abulkhair, *Mol. Diversity*, 2021, **25**(1), 291–306, DOI: 10.1007/s11030-020-10070-w.
50 E. A. Fayed, R. R. E. Eldin, A. B. M. Mehany, A. H. Bayoumi and Y. A. Ammar, *J. Mol. Struct.*, 2021, **1234**, 130159, DOI: 10.1016/j.molstruc.2021.130159.
51 N. Raghav and M. Singh, *Bioorg. Med. Chem.*, 2014, **22**, 4233–4245, DOI: 10.1016/j.bmc.2014.05.037.
52 A. Turky, A. H. Bayoumi, A. Ghiaty, A. S. El-Azab, A. A.-M. Abdel-Aziz and H. S. Abulkhair, *Bioorg. Chem.*, 2020, **101**, 104019, DOI: 10.1016/j.bioorg.2020.104019.
53 M. H. El-Shershaby, A. Ghiaty, A. H. Bayoumi, A. A. Al-Karmalawy, E. M. Husseiny, M. S. El-Zoghbi and H. S. Abulkhair, *Bioorg. Med. Chem.*, 2021, **42**, 116266, DOI: 10.1016/j.bmc.2021.116266.
54 W. S. Hamama, M. E. Ibrahim, A. A. Gooda and H. H. Zoorob, *RSC Adv.*, 2018, **8**, 8484–8515, DOI: 10.1039/C7RA11537G.
55 C. Li, Z. Liu, B. Wang, T. Li and Z. Yang, *Synth. Met.*, 2015, **209**, 273–278, DOI: 10.1016/j.synthmet.2015.08.009.
56 M. Balouiri, M. Sadiki and S. K. Ibnsouda, *J. Pharm. Anal.*, 2015, 1–9, DOI: 10.1016/j.jpha.2015.11.005.
57 E. A. Lindsey, R. J. Worthington, C. Alcaraz and C. Melander, *Org. Biomol. Chem.*, 2012, **10**, 2552, DOI: 10.1039/c2ob06871k.
58 S. Prasad, V. Radhakrishna and T. K. Ravi, *Arab. J. Chem.*, 2019, **12**, 3943–3947, DOI: 10.1016/j.arabjc.2016.03.003.
59 V. Sharma, N. Chitranshi and A. K. Agarwal, *Int. J. Med. Chem.*, 2014, **2014**, 1–31, DOI: 10.1155/2014/202784.
60 Y. Abouelhassan, A. T. Garrison, G. M. Burch, W. Wong, V. M. Norwood and R. W. Huigens, *Bioorg. Med. Chem. Lett.*, 2014, **24**, 5076–5080, DOI: 10.1016/j.bmcl.2014.09.009.
61 T. B. Kakule, D. Sardar, Z. Lin and E. W. Schmidt, *ACS Chem. Biol.*, 2013, **8**, 1549–1557, DOI: 10.1021/cb400159f.
62 F. Collin, S. Karkare and A. Maxwell, *Appl. Microbiol. Biotechnol.*, 2011, **92**, 479–497, DOI: 10.1007/s00253-011-3557-z.
63 B. I. Schweitzer, A. P. Dicker and J. R. Bertino, *FASEB J.*, 1990, **4**, 2441–2452, DOI: 10.1096/fasebj.4.8.2185970.
64 L. Senerovic, D. Opsenica, I. Moric, I. Aleksic, M. Spasić and B. Vasiljevic, *Adv. Exp. Med. Biol.*, 2020, **1282**, 37–69, DOI: 10.1007/5584_2019_428.
65 M. Brvar, A. Perdih, M. Renko, G. Anderluh, D. Turk and T. Solmajer, *J. Med. Chem.*, 2012, **55**, 6413–6426, DOI: 10.1021/jm300395d.
66 D. C. Bensen, J. M. Fortier, S. Akers-Rodriguez and L. W. Tari, Prospecting for broad-spectrum inhibitors of fungal dihydrofolate reductase using a structure guided approach, https://www.rcsb.org/structure/6DRS, (accessed 21 August 2020).
67 I. Kufareva and R. Abagyan, *Methods Mol. Biol.*, 2012, **857**, 231–257, DOI: 10.1007/978-1-61779-588-6_10.
68 C. A. Lipinski, F. Lombardo, B. W. Dominy and P. J. Feeney, *Adv. Drug Delivery Rev.*, 1997, **23**, 3–25, DOI: 10.1016/S0169-409X(96)00423-1.

69 K. El-Adl, M. K. Ibrahim, F. Khedr, H. S. Abulkhair and I. H. Eissa, *Arch. Pharm.*, 2020, **354**(3), 2000219, DOI: 10.1002/ardp.202000219.
70 D. E. V. Pires, T. L. Blundell and D. B. Ascher, *J. Med. Chem.*, 2015, **58**, 4066–4072, DOI: 10.1021/acs.jmedchem.5b00104.
71 A. Beig, R. Agbaria and A. Dahan, *PLoS One*, 2013, **8**, e68237, DOI: 10.1371/journal.pone.0068237.
72 S. Khunt, R. Khedkar, V. Coutinho and E. Tala, *Int. J. Pharm. Res. Scholars*, 2014, **3**, 825–833.
73 H. S. Abulkhair, S. Elmeligie, A. Ghiaty, A. El-Morsy, A. H. Bayoumi, H. E. A. Ahmed, K. El-Adl, M. F. Zayed, M. H. Hassan, E. N. Akl and M. S. El-Zoghbi, *Arch. Pharm.*, 2021, **354**(5), 2000449, DOI: 10.1002/ardp.202000449.
74 K. El-Adl, H. Sakr, S. S. A. El-Hddad, A. G. A. El-Helby, M. Nasser and H. S. Abulkhair, *Arch. Pharm.*, 2021, **354**(7), 2000491, DOI: 10.1002/ardp.202000491.
75 A. Abo Elmaaty, M. I. A. Hamed, M. I. Ismail, E. B. Elkaeed, H. S. Abulkhair, M. Khattab and A. A. Al-Karmalawy, *Molecules*, 2021, **26**(12), 3772, DOI: 10.3390/molecules 26123772.
76 A. Turky, A. H. Bayoumi, F. F. Sherbiny, K. El-Adl and H. S. Abulkhair, *Mol. Diversity*, 2021, **25**(1), 403–420, DOI: 10.1007/s11030-020-10131-0.
77 A.-G. A. El-Helby, R. R. A. Ayyad, M. F. Zayed, H. S. Abulkhair, H. Elkady and K. El-Adl, *Arch. Pharm.*, 2019, **352**(5), 1800387, DOI: 10.1002/ardp.201800387.

